Article

Congestion-Aware Rideshare Dispatch for Shared Autonomous Electric Vehicle Fleets

Chenn-Jung Huang [1,2,*] **, Kai-Wen Hu** [2] **and Cheng-Yang Hsieh** [1]

1   Department of Computer Science & Information Engineering, National Dong Hwa University, Shoufeng, Hualien 974301, Taiwan
2   Department of Electrical Engineering, National Dong Hwa University, Shoufeng, Hualien 974301, Taiwan
*   Correspondence: cjhuang@gms.ndhu.edu.tw

Abstract: The problem of traffic congestion caused by the fast-growing travel demands has been getting serious in urban areas. Meanwhile, the future of urban mobility has been foreseen as being electric, shared, and autonomous. Accordingly, the routing and charging strategies for fleets of shared autonomous electric vehicles (SAEVs) need to be carefully addressed to cope with the characteristics of the rideshare service operation of the SAEV fleets. In the literature, much work has been done to develop various traffic control strategies for alleviating the problem in urban traffic congestion. However, little research has proposed effective solutions that integrate the route of charging strategies for SAEV fleets with the urban traffic congestion problem. In this regard, this work presents an integrated framework that tackles the route and charging of SAEV fleets as well as the urban traffic congestion prevention issues. Notably, our contribution in this work not only proposes a joint solution for the problems of the urban traffic congestion control and rideshare dispatch of SAEV fleets, but also fills the gap of the routing and charging strategies for mixed privately owned EVs (PEV) and SAEV fleets in the literature. A general optimization framework is formulated, and effective heuristics are proposed to tackle the above-mentioned problems in this work. The feasibility and effectiveness of the proposed algorithms were evaluated through four different scenarios in the simulation. After applying the proposed algorithms, the traffic volumes of the oversaturated main arterial road were diverted to other less busy road sections, and the traveling times of EV passengers were decreased by 28% during peak periods. The simulation results reveal that the proposed algorithms not only provide a practical solution to prevent the problem in urban traffic congestion during rush hours, but also shorten the travel times of EV passengers effectively.

Keywords: congestion control; optimization; shared autonomous electric vehicle; rideshare; routing and charging

1. Introduction

Urbanization is an unavoidable trend in most of the countries in the world. It was projected that more than two-thirds of the world population will live in urban areas by 2050 [1]. However, the traffic congestion problem caused by the fast-growing travel demands has been getting serious in urban areas. The contradiction between the mass number of vehicles and the limited road resource should be resolved by the local governments in due course. Although various traffic management methods have been proposed to alleviate the traffic jams in urban areas during rush hours, the huge traffic volumes during peak periods resulted from the overwhelming increase in privately owned vehicles are still causing a large amount of economic losses and a negative impact on the future development of an urban area.

With the increasing popularity of electric vehicles (EVs), the future of urban mobility has been foreseen as being electric, shared, and autonomous [2]. This kind of future transportation can be potentially an effective approach for alleviating the urban congestion problem when these new mobility technologies are widely accepted by the public [3].

Much work has been done in the recent literature to develop various traffic control strategies for alleviating the metropolitan traffic congestion problem. However, the vast majority of studies focused on real-time traffic congestion control, and few studies addressed the issue of urban traffic congestion prevention during commute times. Accordingly, congested traffic caused by overwhelmed volumes of vehicles entering popular road sections during peak hours cannot be alleviated effectively in the metropolitan area.

Although the issues of routing and charging strategies for conventional EVs or SAEVs have been addressed in the literature, the joint problem of urban congestion prevention and routing/charging strategies for SAEV fleets needs to be revised to fit the characteristics of the rideshare service operation of the SAEV fleets. Since the urban traffic congestion problem should be handled in an effective way to keep the urban areas developing in a healthy pace, the issue of routing and charging strategies for SAEV fleets that offer rideshare services should be bundled with the traffic congestion solution to cope with the outlook of future urban transportation. In order to deal with the urban traffic congestion problem effectively, this work proposes an integrated framework of traffic congestion control and cooperative rideshare dispatch of SAEV fleets to fill the gap in the literature. EVs first book their routes before departure to ensure that they can be allowed to drive on the busy roads during rush hours. Real-time traffic volume surveillance is operated at the designated busy road sections, and flow redistribution is manipulated to reduce the traffic loads of busy roads. Notably, a rideshare coordinator is employed to assist a rideshare passenger in finding any available rideshare route from all SAEV fleets. The following section reviews recent work on traffic congestion control strategies and routing/charging of SAEVs. Section 3 presents the detailed description of the proposed approach. The effectiveness of the developed approach is assessed in Section 4. Section 5 concludes with a discussion.

2. Literature Review

As mentioned above, much work in the literature developed traffic control algorithms to alleviate the metropolitan traffic congestion problem. Numerous researchers proposed traffic signal control schemes to tackle the traffic congestion problem. To mention a few, Joo et al. proposed a traffic signal control system to maximize the number of vehicles crossing a road intersection and balanced the signals between roads by using the Q-learning technique [4]. Kumar et al. proposed a dynamic and intelligent traffic light control system that takes real-time traffic information as the input and adjusts the traffic light duration dynamically [5]. The deep reinforcement learning technique was employed to switch the traffic lights in different phases, and the fuzzy inference system was used to minimize the average waiting time of high priority vehicles. Rasheed et al. tackled the problems of the recurring traffic congestion caused by high traffic volume and non-recurring traffic congestion caused by disturbance using a deep Q-network approach [6]. An extended multi-agent deep Q-network was presented in order to solve multi-agent problems by coordinating their actions via information exchange among deep Q-network agents. Wang et al. proposed an adaptive linear quadratic regulator control strategy for traffic signal control [7]. Their method not only can improve network-wide traffic operations in terms of reduced traffic delay and energy consumption, but also is more computationally feasible than the existing centralized signal control methods. Du et al. proposed a coupled vehicle-signal control method to optimize mixed traffic flow at signalized intersections [8]. The traffic signal timing and connected and automated vehicle (CAV) driving trajectory are established to reduce vehicles' delay time, and fuel consumption.

Some researchers developed predictive control algorithms to address the congestion control issue in recent literature. Hou and Lei proposed an adaptive predictive control scheme for perimeter control and route guidance of multi-region urban traffic systems [9]. They used the input and output data of the controlled multi-region urban traffic systems to design the perimeter control and route guidance strategies. Li et al. [10] first derived the data models of multi-region urban traffic network and proposed a distributed model-free

adaptive predictive control method to avoid the model mismatch problem and decrease the computational burden of traditional mathematical traffic models. Zhang et al. presented a Spark cloud computing-based traffic network flow control based on the mechanism of model predictive control (MPC) [11]. A two-level hierarchical parallel genetic algorithm was adopted to reduce the overhead of online computation. Hosseinzadeh et al. proposed an emergency vehicle-prioritized traffic control mechanism to mitigate traffic congestion of interconnected signaled lanes [12]. The cell transmission model was integrated with MPC to ensure that emergency vehicles traverse multiple intersections efficiently and in a timely manner. Zuo et al. proposed an improved particle-swarm-optimization-based MPC method to solve the vehicle planning and tracking problem [13]. A pseudo velocity planning algorithm was adopted to handle the constraints on both traffic lights and motion obstacles. Wang and Wang proposed a real-time dynamic route optimization algorithm using predictive control [14]. Their algorithm switched the route among different static shortest routes based on the dynamic road conditions.

Aside from the above-mentioned traffic control heuristics, the strategy of congestion pricing was also adopted in some metropolitan areas recently to alleviate traffic congestion problems. Chen et al. adopted a cumulative prospect theory in a congestion pricing plan in Melbourne traffic network [15]. The concepts of level of service and demand management were incorporated into a single pricing scheme. Baghestani et al. investigated changes of travel behavior in response to cordon pricing in Manhattan, New York [16]. Several pricing schemes with variable cordon charging fees were proposed, and their findings suggest that cordon pricing can improve traffic congestion and air quality effectively. Genser and Kouvelas evaluated the feasibility of implementing a congestion pricing strategy in Zurich [17]. Their method trained neural network models to predict generalized costs and derive optimal pricing functions.

Abulibdeh's study applied optimized tolling in Abu Dhabi city and investigated the public acceptability of congestion pricings, including high-occupancy toll lanes, and cordon pricing lanes and cordon pricing [18]. It was observed that the driver's age and her/his income, journey urgency level, distance traveled, driving speed, employment and vehicle ownership, and tolls are key factors in determining the public acceptance of high-occupancy toll lanes. Baghestani et al. applied cordon pricing in New York City and observed three key factors, including traffic, public transportation access, and environmental concerns [19]. Their study showed that cordon pricing in Manhattan's Central Business District considerably improved traffic and environmental metrics for the population inside the cordon area without severe impacts in other boroughs. Guo et al. investigated how congestion pricing and reward policies impacted the vehicle drivers' behavior in Beijing. [20]. Their findings from the model estimation and descriptive statistics showed that the adoption of pricing policy may potentially bring new add some economic burden to migrant car travelers. Abbasi et al. investigated the public acceptability of the congestion pricing zone in Tehran using 1388 stated preference questionnaires [21]. It was observed that a resident preferred driving her/his private car rather than taxis and motorcycles, owing to the reduced congestion pricing cost during the off-peak hours.

As mentioned in Section 1, it is very likely that shared autonomous electric vehicles (SAEVs) will be an important means of transportation to mitigate urban traffic congestion in the future. Accordingly, research issues related to the dispatch of rideshare services supported by SAEVs fleets also attracted researchers' attention in the recent literature [22]. To name a few, Huo et al. proposed a mixed-integer program to formulate the ridesharing dispatch of SAEVs [23]. The uncertain demand and vehicle upgrade policy problems were addressed in their solution. Haliem et al. developed a demand-aware rideshare matching and route planning algorithm [24]. The deep reinforcement learning technique was employed to dispatch SAEVs to the areas of high demand. Kim et al. presented an idle vehicle relocation algorithm using the deep learning technique [25]. Their algorithm first predicted passenger demand for shared vehicles and then relocated the idle SAEVs based on the demand prediction. Levin presented a rideshare dispatch policy of SAVEs

that considered the recharging of EVs and the integration with public transit [26]. Whether a demand rate can be served by a given fleet size was also analyzed in their work. Li et al. proposed a real-time SAEV rideshare dispatch method by modeling the dispatch problem as a stochastic queuing network [27]. Lyapunov optimization techniques were used in their model to ensure the stability of customers' waiting times.

Recently, some researchers also proposed routing and charging strategies for SAEVs in the literature. Dai et al. presented a reservation system for autonomous taxi ride sharing [28]. Their work considers the practical features of both the power and transportation systems, including taxi type, taxi path, feet size, depot location, and energy consumption problem. Dean et al. studied the interaction between a fleet of SAEVs servicing on-demand transportation requests and the electric power network [29]. Their study shortened rider wait times, reduced extra traversing time of SAEVs due to repositioning or charging, and improved average daily trips per vehicle and charging queues. Melendez et al. presented a methodology that yields optimal operational strategies for a SAEV fleet to maximize gross profit for the system [30]. Their model considers a number of practical features of both the power and transportation systems. Alqahtani et al. addressed the problem of routing and electricity scheduling of SAEVs using the decentralized Markov decision process model and a multi-agent reinforcement learning algorithm [31]. Their solution aimed to provide efficient solutions that can promptly respond to system dynamics and uncertainties. Zhang et al. studied the uncertain routing optimization problem of SAEVs with charging schedules in [32]. They designed a label setting algorithm to determine feasible routes with charging schedules that take acceptable pricing into consideration. In a case study reported in [33], the authors proposed a smart charging algorithm using trip patterns from the regional travel demand model and local energy prices.

The research topics and used methods of the above-mentioned recent literature are summarized in Table 1. It can be seen from Table 1 that no integrated solution for tackling the joint problem of urban traffic congestion and routing/charging of SAEVs has been proposed in the literature.

Table 1. The summary of related work.

| Ref.	Year	Research Topics	Used Methods
[4]	2020	Urban traffic congestion control	Traffic signal control using reinforcement learning
[5]	2021	Urban traffic congestion control	Traffic signal control using deep reinforcement learning and fuzzy inference system
[6]	2020	Urban traffic congestion control	Traffic signal control using deep Q-network
[7]	2022	Urban traffic congestion control	Traffic signal control using adaptive linear quadratic regulator control
[8]	2021	Urban traffic congestion control	Optimize mixed traffic flow using a coupled vehicle-signal control method
[9]	2022	Urban traffic congestion control	Perimeter control and route guidance strategies using adaptive predictive control
[10]	2022	Urban traffic congestion control	Optimize traffic flow using a distributed model-free adaptive predictive control method
[11]	2022	Urban traffic congestion control	Traffic flow predictive control using genetic algorithm and MPC
[12]	2022	Urban traffic congestion control	Emergency vehicle-prioritized traffic control using cell transmission model and MPC
[13]	2021	Urban traffic congestion control	Vehicle planning and tracking using improved particle swarm optimization and MPC
[14]	2020	Urban traffic congestion control	Vehicle route selection using predictive control
[15]	2021	Urban traffic congestion control	Congestion pricing using a cumulative prospect theory

Table 1. *Cont.*

Ref.	Year	Research Topics	Used Methods
[16]	2020	Urban traffic congestion control	Congestion pricing schemes with variable cordon charging fees
[17]	2022	Urban traffic congestion control	Congestion pricing using neural network models
[18]	2022	Urban traffic congestion control	Survey of public acceptability of different congestion pricings
[19]	2022	Urban traffic congestion control	Investigation of the impact of cordon pricing on traffic, public transportation access, and environmental concerns
[20]	2022	Urban traffic congestion control	Investigation of how urban residents' behaviors respond with congestion pricing
[21]	2022	Urban traffic congestion control	Investigation of public acceptability of congestion pricing zone
[23]	2022	Ridesharing dispatch of SAEVs	Formulation of ridesharing dispatch using mixed-integer program
[24]	2021	Ridesharing dispatch of SAEVs	Rideshare matching and route planning using deep reinforcement learning
[25]	2022	Ridesharing dispatch of SAEVs	Idle vehicle relocation using deep learning
[26]	2022	Ridesharing dispatch of SAEVs	Rideshare dispatch considering the recharging of EVs and the integration with public transit
[27]	2021	Ridesharing dispatch of SAEVs	Rideshare dispatch using stochastic queuing and Lyapunov optimization
[28]	2022	Routing & charging for SAEVs	Reservation system considering practical features of the power and transportation systems
[29]	2022	Routing & charging for SAEVs	The study of the interaction between SAEVs servicing on-demand transportation requests and the electric power network
[30]	2022	Routing & charging for SAEVs	Optimal operational strategies for SAEVs to maximize gross profit
[31]	2022	Routing & charging for SAEVs	Routing and electricity scheduling of SAEVs using decentralized Markov decision process model and a multi-agent reinforcement learning
[32]	2022	Routing & charging for SAEVs	Uncertain routing optimization problem of SAEVs with charging schedules
[33]	2020	Routing & charging for SAEVs	A smart charging algorithm using trip patterns from the regional travel demand model and local energy prices

3. Coordinated Urban Traffic Congestion Control for Mixed PEVs and SAEV Fleets

Figure 1 shows the integrated framework of traffic congestion control and cooperative rideshare dispatch of SAEV fleets proposed in this work. This work enforces the limitation of traffic volumes on busy roads in an urban area during peak periods. In other words, congestion control is operated at busy roads to keep the traffic smooth, whereas flow redistribution is manipulated at the rest of the road sections in an urban area to distribute the vehicles in balance over local roads at which congestion control is not put into practice.

Both PEVs and SAEV fleets are encouraged to book their routes before departure to ensure the allowance to drive on the busy roads during rush hours. The ratio for the number of the admitted PEVs to that of SAEVs is determined by the metropolitan traffic monitoring module as illustrated at the upper-right area of Figure 1. The system operator of each SAEV fleet can use the rideshare booking module as illustrated at the lower-left area of Figure 1 to handle the route booking for a SAEV, whereas the driver of a parked PEV can schedule their trips in advance by using the route booking module as given at the lower-middle area of Figure 1. In this work, the route booking of a PEV or SAEV fleet is assisted by the well-known support vector regressions in determining the time taken for a route [34]. Since it is also possible for a PEV user to take an unexpected trip right away, the on-road routing module as illustrated at the lower-right area of Figure 1 is used to handle

the unplanned trips of PEV users. The ratio of the number of PEVs booking ahead to that of PEV taking unplanned trips is set by the system operator.
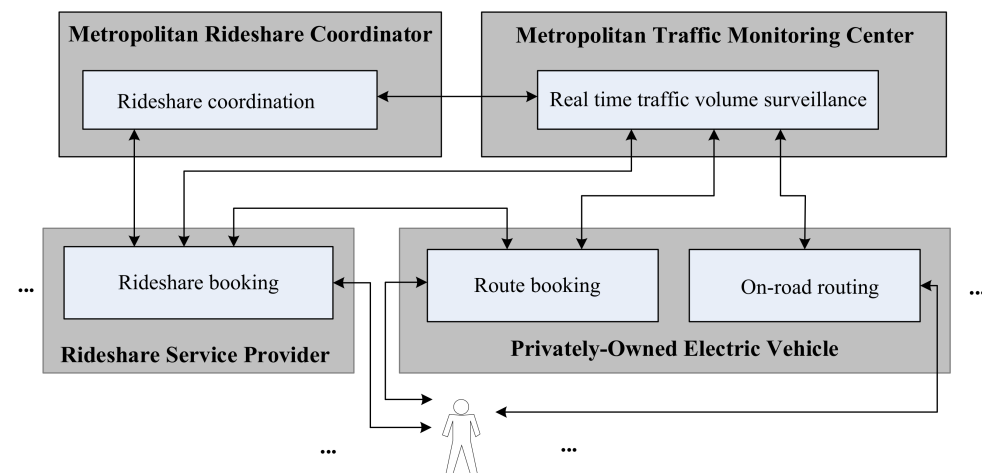
Figure 1. Integrated framework of traffic congestion prevention and cooperative rideshare dispatch of SAEV fleets.

Real-time traffic volume surveillance is operated at the designated busy road sections, such as an arterial road to keep the traffic smooth, and flow redistribution is manipulated at the rest of the road sections to distribute the EV in balance over local roads where congestion control is not put into practice. Once the booked route of a PEV/SAEV is computed, the metropolitan traffic monitoring module will receive the route-booking request from the PEV/SAEV and check if all road sections on the route are available. As the traffic congestion in urban areas during rush hours might be serious to delay the original estimated time arriving at busy road sections, the metropolitan traffic monitoring center will be informed of all schedule changes of EV bookings and refresh the reservation records at all road sections accordingly. Notably, congestion control is not enforced in parts of local roads, and the PEVs/SAEVs that are declined to take the route on some busy road sections can still take use of these local roads to reach their destinations during rush hours. The flow redistribution operation is enforced on the local roads to assign EVs to alternative local road sections to balance the traffic flows.

It is very likely a PEV user cannot be admitted to take popular routes during peak periods, owing to the limited quota set for PEVs. Thus, a PEV user can use an APP to request a rideshare service that satisfies their requirements. If all members of the requested SAEV fleet are on duty during the time period of the requester's trip, the SAEV fleet will then inform the rideshare coordinator upstream. The module as illustrated at the upper-left area of Figure 1 will be activated by the rideshare coordinator to find any available rideshare route from other cooperative SAEV fleets. In the case of no rideshare services that fits the requester's demand, the requester will be informed by the rideshare coordinator to take public transportation instead. Notably, this work assumes the government will offer some incentives for commuters to take the rideshare services, such as enforcing congestion pricing for the PEVs driving on the busy road sections during rush hours. Thus, most of commuters are willing to choose to commute to work by rideshare to save the expenses.

Since PEVs or SAEVs might not reach some pre-routed busy road sections on time during traffic jams, the metropolitan traffic monitoring module can then assign these busy road sections to the demanding vehicles that fail to book beforehand instead. Accordingly, a moving PEV employs the on-road routing APP as shown at the lower-right area of Figure 1 to find better routes that fit their needs, along with the un-booked PEVs that are about to leave for their destination.

It can be seen from the literature review that the charging scheduling for a SAEV fleet should be carefully arranged because it is inappropriate to incur more delay for

the rideshare passengers, owing to the battery charging of a SAEV. This work assumes three battery charging options available for EV battery charging. Most PEVs can charge their batteries during parking after they arrive at their destinations. However, the most appropriate charging option during duty of a SAEV fleet should be dynamic wireless charging [35] because the battery can be recharged while an EV drives on the road section paved with a wireless charging pad. On the contrary, conventional plug-in charging [36] or battery-swapping facilities [37] can be taken as the alternatives to the electric road charging for a member of a SAEV fleet while it is off duty because the charging cost is much less than the electric road charging.

The implementation details of the components employed in the proposed framework are given as follows.

3.1. Route Booking of a PEV Prior to Its Trip

This module is employed by a PEV user to set up the route of a scheduled trip. The state of charge (SOC) of PEV battery is checked along with the route planning to ensure the PEV can reach the destination without depleting its battery. Up to three charging options can be chosen for a PEV user, including plug and charge, battery exchange, or on-road wireless charging on an electric road, if the battery electricity is inadequate to arrive at the destination. A plug and charge option suits the PEV user that cannot charge the battery at home/work if the number of the plug and charge slots is limited at the building at which the PEV is parked. However, electric road charging or battery exchange will be preferred by a PEV user if she/he is pressed for time to reach the destination.

Once this module is activated, a list consisting of K candidate routes that fits the preferences of the PEV user is derived by

$$
\begin{aligned}
\arg \underset{l}{\text{Min}} \Big\{ & \omega_1^l \cdot \sum_{1 \le i < h_l} sl_{c_i^l, c_{i+1}^l} + \omega_2^l \cdot \sum_{1 \le i < h_l} cp_{c_i^l, c_{i+1}^l}\left(rt_{c_i^l}\right) + \omega_3^l \cdot \left(rt_{c_{h_l}^l} - rt_{c_1^l}\right) + \omega_4^l \\
& \cdot \Bigg[\sum_{1 \le i < h_l} \phi_{c_i^l} \cdot RP_{c_i^l}\left(rt_{c_i^l}\right) \cdot pcp_{c_i^l} \cdot ct_{c_i^l} \\
& + \sum_{1 \le i < h_l} \theta_{c_i^l, c_{i+1}^l} \cdot WP_{c_i^l, c_{i+1}^l}\left(rt_{c_i^l}\right) \cdot wcp_{c_i^l, c_{i+1}^l} \cdot SD_{c_i^l, c_{i+1}^l}\left(rt_{c_i^l}\right) \\
& + \sum_{1 \le i < h_l} \psi_{c_i^l} \cdot RP_{c_i^l}\left(rt_{c_i^l}\right) \cdot \left(SOC^{max} - SOC_{c_i^l}^l\right) \Bigg] \Big\}, \; 1 \le l \le K
\end{aligned}
\tag{1}
$$

subject to

$$
K = \min\left[K^{max}, \underset{l}{\arg\min}\left(rt_{c_{h_{l+1}}^{l+1}} > rt_{Dst}^{max}\right) \right],
\tag{2}
$$

$$
c_1^l = Org, \; c_{h_l}^l = Dst, \; 1 \le l \le K
\tag{3}
$$

$$
rt_{c_1^l} = rt_{Org}, \; 1 \le l \le K
\tag{4}
$$

$$
sl_{c_i^l, c_{i+1}^l} = \infty, \; \text{if } \xi_{c_i^l, c_{i+1}^l}\left(rt_{c_i^l}\right) = 1, \; 1 \le i < h_l, \; 1 \le l \le K
\tag{5}
$$

$$
\sum_{1 \le i < h_l} sl_{c_i^l, c_{i+1}^l} \le \sum_{1 \le i < h_{l+1}} sl_{c_i^{l+1}, c_{i+1}^{l+1}} \; 1 \le l < K
\tag{6}
$$

$$
\begin{aligned}
&rt_{c_{i+1}^l} = rt_{c_i^l} + \left(1 - \phi_{c_i^l}\right) \cdot \left(1 - \psi_{c_i^l}\right) \cdot ID_{c_i^l, c_{i+1}^l}\left(rt_{c_i^l}\right) + SD_{c_i^l, c_{i+1}^l}\left(rt_{c_i^l}\right) + \phi_{c_i^l} \cdot ct_{c_i^l} + \psi_{c_i^l} \cdot BSD_{c_i^l}\left(rt_{c_i^l}\right), \\
&1 \le i < h_l, 1 \le l \le K
\end{aligned}
\tag{7}
$$

$$
\begin{aligned}
SoC_{c_{i+1}^l} = {} & SoC_{c_i^l} + \eta \cdot \phi_{c_i^l} \cdot pcp_{c_i^l} \cdot ct_{c_i^l} + \eta \cdot \theta_{c_i^l, c_{i+1}^l} \cdot wcp_{c_i^l, c_{i+1}^l} \cdot SD_{c_i^l, c_{i+1}^l}\left(rt_{c_i^l}\right) + \\
& \psi_{c_i^l} \cdot \left(SOC^{max} - SoC_{c_i^l}\right) - ap \cdot sl_{c_i^l, c_{i+1}^l},
\end{aligned}
\tag{8}
$$

$$1 \leq i < h_l, 1 \leq l \leq K$$

$$0 \leq ct_{c_i^l} \leq ct_{c_i^l}^{max}, \text{ if } \phi_{c_i^l} = 1 \tag{9}$$

$$SOC^{min} \leq SoC_{c_i^l} \leq SOC^{max}, 1 \leq i \leq h_l, 1 \leq l \leq K \tag{10}$$

$$\sum_{1 \leq i < h_l} \left(\phi_{c_i^l} + \theta_{c_i^l, c_{i+1}^l} + \psi_{c_i^l} \right) \geq 1, \text{ if } SoC_{c_1^l} - ap \cdot \sum_{1 \leq i < h_l} sl_{c_i^l, c_{i+1}^l} < SOC^{min}, \tag{11}$$

$$1 \leq l \leq K$$

$$0 \leq \eta \leq 1 \tag{12}$$

The parameters adopted in the equations shown above are defined as follows:

- Each of the four weights ω_1^l, ω_2^l, ω_3^l; and ω_4^l is used to indicate the impact of the corresponding parameter on the minimization objective. Notably, the value of ω_4^l is clear to zero if there is no shortage of PEV battery capacity before reaching the destination.

- *Org* and *Dst* denote the start and end points, respectively. c_1^l, c_i^l, and $c_{h_l}^l$ represent the origin, the ith intersection, and the final destination of the route indexed by l, respectively. $sl_{c_i^l, c_{i+1}^l}$ denotes the length of the road section connecting c_i^l and c_{i+1}^l, whereas $\sum_{1 \leq i < h_l} sl_{c_i^l, c_{i+1}^l}$ is the total length of the lth route. $rt_{c_i^l}$ is the arrival time of the PEV at c_i, whereas rt_{Org} and rt_{Dst}^{max} are the departure time at the origin and the deadline to reach the destination, respectively. K stands for the number of candidate routes that are kept by the PEV user, whereas K^{max} is the preset maximal number of candidate route records saved by the PEV user.

- $cp_{c_i^l, c_{i+1}^l} \left(rt_{c_i^l} \right)$ indicates the congestion pricing policy enforced on the road section between c_i^l and c_{i+1}^l at the time $rt_{c_i^l}$. $cp_{c_i^l, c_{i+1}^l} \left(rt_{c_i^l} \right)$ is set to zero during off-peak periods. $SD_{c_i^l, c_{i+1}^l}(t)$ denotes the time of the PEV while it takes the road section between c_i^l and c_{i+1}^l at time t, whereas $ID_{c_i^l, c_{i+1}^l}(t)$ stands for the delay of the PEV while it reaches the intersection c_i at time t. Notably, both $ID_{c_i^l, c_{i+1}^l}(\cdot)$ and $SD_{c_i^l, c_{i+1}^l}(\cdot)$ are predicted by using SVRs owing to its effectiveness of travel time prediction in the literature.

- SOC^{max} and SOC^{min} represent the maximal and minimal PEV battery capacity, respectively. $SoC_{c_i^l}$ represents the PEV battery capacity when the PEV reaches c_i^l. Notably, all plug and charge stations and battery exchange services are located at intersections in this work. The binary flags $\phi_{c_i^l}$, $\psi_{c_i^l}$ and $\theta_{c_i^l, c_{i+1}^l}$ are used to indicate if a battery charging service is provided by a plug & charge station indexed by c_i^l, a battery exchange service indexed by c_i^l, or an electric road charging between c_i^l and c_{i+1}^l, respectively. The flag of a chosen charging service is set to one. Otherwise, it is clear to zero. Accordingly, the PEV battery capacity after the PEV reaches intersection c_{i+1}^l is computed in Equation (8), regardless of whether the PEV battery is charged after the PEV passes c_i^l.

- $RP_{c_i^l}(t)$ denotes the charging cost of the plug and charge or battery exchange service indexed by c_i^l at time t, whereas $WP_{c_i^l, c_{i+1}^l}(t)$ denotes that of the electric road charging over the section connecting c_i^l and c_{i+1}^l at time t. $pcp_{c_i^l}$ is the battery charging power/sec for the plug and charge station indexed by c_i^l, whereas $wcp_{c_i^l, c_{i+1}^l}$ is the battery charging power/sec for the electric road charging over the section connecting c_i^l and c_{i+1}^l, respectively. $ct_{c_i^l}$ and $ct_{c_i^l}^{max}$ denote the actual and the maximal battery charging time of the PEV at the plug and charge station c_i^l, respectively. $SD_{c_i^l, c_{i+1}^l}(t)$ stands for the charging time on the electric road, which is the time that the PEV drives

through the section connecting c_i^l and c_{i+1}^l. $BSD_{c_i^l}(t)$ stands for the time that the PEV takes the battery exchange service provided by c_i^l at time t.

- ap is the PEV battery power consumption per kilometer, whereas η denotes the charging efficiency of the PEV battery. The binary flag $\xi_{c_i^l,c_{i+1}^l}\left(rt_{c_i^l}\right)$ is used to control the traffic of the road section connecting c_i^l and c_{i+1}^l at the time $rt_{c_i^l}$. $\xi_{c_i^l,c_{i+1}^l}\left(rt_{c_i^l}\right)$ is set to one if a PEV is prohibited to enter the road section connecting c_i^l and c_{i+1}^l during peak periods. Otherwise, this flag is clear to zero.

The four optimization objectives specified in Equation (1) are as follows. The first objective is the distance traveled by the PEV, the second is the congestion fee to be paid by the PEV owner, and the third and fourth are the travel time and charging cost of the PEV, respectively. The weight of each optimization objective is the priority of the corresponding objective. In order to reduce the computational burden, we first use Yen's algorithm [38] to select at most K^{max} shortest routes. Then the top K candidate routes are calculated from the four optimized target values in Equation (1) based on the constraints of Equations (2) through (12).

At this moment, at most K sorted candidate routes are generated by the above equations. This module then picks up the most favorite route of the PEV by

$$cm_{c_i^l,c_{i+1}^l} = \begin{cases} 0 & \text{if } \pi\cdot\rho_{c_i^l,c_{i+1}^l}^{rb}\left(\tau_{c_i^l,c_{i+1}^l}\right) + (1-\pi)\cdot\rho_{c_i^l,c_{i+1}^l}^{rr}\left(\tau_{c_i^l,c_{i+1}^l}\right) < \pi\cdot\rho_{c_i^l,c_{i+1}^l}^{rb,\,max}\left(\tau_{c_i^l,c_{i+1}^l}\right) + \\ & \quad (1-\pi)\cdot\rho_{c_i^l,c_{i+1}^l}^{rr,max}\left(\tau_{c_i^l,c_{i+1}^l}\right),\ \tau_{c_i^l,c_{i+1}^l} \le rt_{c_i^l} < \tau_{c_i^l,c_{i+1}^l} + \Delta \\ 1 & \text{Otherwise} \end{cases} \quad (13)$$

$$ci^l = \sum_{1 \le i < h_l} cm_{c_i^l,c_{i+1}^l},\ 1 \le l \le K \quad (14)$$

where the binary flag π is set to one if the booking is made in advance. Otherwise, it is set to zero when the EV is about to head for the destination without making reservation first. This work estimates the traffic density of a road section within a fixed interval Δ. $\rho_{c_i^l,c_{i+1}^l}^{rb}\left(\tau_{c_i^l,c_{i+1}^l}\right)$ and $\rho_{c_i^l,c_{i+1}^l}^{rr}\left(\tau_{c_i^l,c_{i+1}^l}\right)$ denote the updated traffic density for the route bookings of PEVs and that for on-road routings of PEVs at the road section connecting c_i^l and c_{i+1}^l during the future interval starting at time $\tau_{c_i^l,c_{i+1}^l}$, respectively. $\rho_{c_i^l,c_{i+1}^l}^{rb,max}\left(\tau_{c_i^l,c_{i+1}^l}\right)$ and $\rho_{c_i^l,c_{i+1}^l}^{rr,max}\left(\tau_{c_i^l,c_{i+1}^l}\right)$ denote the maximal traffic density allowed for route bookings of PEVs and that allowed for on-road routings of PEVs, respectively. The values of $\rho_{c_i^l,c_{i+1}^l}^{rb,max}\left(\tau_{c_i^l,c_{i+1}^l}\right)$ and $\rho_{c_i^l,c_{i+1}^l}^{rr,max}\left(\tau_{c_i^l,c_{i+1}^l}\right)$ are set to very large natural numbers if congestion control is not enforced on the road section between c_i^l and c_{i+1}^l. Meanwhile, the binary flag $cm_{c_i^l,c_{i+1}^l}$ is clear to zero if the road section between c_i^l and c_{i+1}^l is not congested. Otherwise, it is set to one. ci^l indicates whether the lth route is not congested. Accordingly, all the routes with this variable equal to zero are treated as qualified routes for the PEV.

This module then chooses the qualified route with the smallest index l for the PEV and confirms with the metropolitan traffic monitoring center if such a congestion-free route is found. Meanwhile, the rejected routes can be used as candidate alternative routes after the PEV starts moving. The records of the congested routes are kept at the cellphone of the PEV user for future reference. These records are downloaded into the on-board unit (OBU) of the PEV after the PEV start moving. Notably, if no suitable route is available owing to traffic congestion, a rideshare service alternative will be suggested to the PEV driver.

The step-by-step description of the algorithm is given below:

Step 1: Apply Yen's algorithm [38] select at most K^{max} shortest routes of the PEV.

Step 2: Use Equations (1) through (12) to select top K sorted candidate routes.

Step 3: Use Equations (13) and (14) to select the candidate route with the smallest index l.

Step 4: If a candidate route is found, check with the metropolitan traffic monitoring center.

Step 5: If the selected candidate route is rejected by the metropolitan traffic monitoring center, remove the selected route from the candidate route list and go to Step 3.

Step 6: If no suitable route is available, recommend the PEV user an alternative rideshare service.

3.2. On-Road Routing of a Moving PEV

This module is installed at the OBU of the PEV. At the end of each fixed short interval, a moving PEV can request for the real-time traffic condition. In the case that the PEV cannot arrive at any of reserved road sections on time, the PEV will notify the metropolitan traffic monitoring center of the newly estimated arrival times at the rest of the reserved road sections on the trip.

This module checks the deviation between the updated times for a moving PEV reaches intersections ahead and the times estimated during the route reservation stage:

$$rt'_{c_1^l} = rt_{Cur} + SD_{c_0^l, c_1^l}\left(rt'_{c_0^l}\right) \cdot \frac{sl_{Cur, c_1^l}}{sl_{c_0^l, c_1^l}} \tag{15}$$

$$rt'_{c_{i+1}^l} = rt'_{c_i^l} + \left(1 - \phi_{c_i^l}\right) \cdot \left(1 - \psi_{c_i^l}\right) \cdot ID_{c_i^l, c_{i+1}^l}\left(rt'_{c_i^l}\right) + SD_{c_i^l, c_{i+1}^l}\left(rt'_{c_i^l}\right) + \phi_{c_i^l} \cdot ct_{c_i^l} + \psi_{c_i^l} \cdot BSD_{c_i^l}\left(rt'_{c_i^l}\right), 1 \leq i < v(l) \tag{16}$$

$$df_{c_i^l, c_{i+1}^l} = \begin{cases} 1, & \text{if } \left|rt_{c_i^l} - rt'_{c_i^l}\right| > \delta_{c_i^l, c_{i+1}^l}, \ 1 \leq i < v(l) \\ 0, & \text{Otherwise} \end{cases} \tag{17}$$

where l is the index of the PEV's current route, c_0^l, c_1^l, and $c_{v(l)}^l$ denote the index of the intersection just passed, that of the closest intersection ahead on the route, and that of the destination, respectively. Cur and rt_{Cur} represent the current location of the PEV and the current time, respectively. $rt'_{c_i^l}$ denotes the updated time that the PEV reaches the intersection c_i^l. sl_{Cur, c_i^l} stands for the distance between the current location and the closest intersection ahead. The binary flag $df_{c_i^l, c_{i+1}^l}$ is used to indicate whether the updated arrival time and the original time estimated during route booking is larger than a preset threshold $\delta_{c_i^l, c_{i+1}^l}$. In the case of any discrepancy between the new predicted time, where the original estimated time is larger than the preset threshold, the metropolitan traffic monitoring center will be informed of the schedule change.

Next, the PEV user can check whether any preferred route that was rejected during the route booking is now available owing to the schedule change of some other EV(s). This module first uses Equations (15) and (16) to update the arrival times of the intersections on a preferred route which was rejected earlier. Then the availability of the candidate route can be computed by

$$sa_{c_i, c_{i+1}} = \begin{cases} 0 & \text{if } \rho^{rr}_{c_i^\sigma, c_{i+1}^\sigma}\left(\tau_{c_i^\sigma, c_{i+1}^\sigma}\right) < \rho^{rr, max}_{c_i^\sigma, c_{i+1}^\sigma}\left(\tau_{c_i^\sigma, c_{i+1}^\sigma}\right), \\ & 1 \leq i < v(\sigma), 1 \leq< l, \ \tau_{c_i^\sigma, c_{i+1}^\sigma} \leq rt'_{c_i^\sigma} < \tau_{c_i^\sigma, c_{i+1}^\sigma} + \Delta \\ 1 & \text{Otherwise} \end{cases} \tag{18}$$

$$ra^\sigma = \sum_{1 \leq i < v(\sigma)} sa_{c_i^\sigma, c_{i+1}^\sigma}, 1 \leq \sigma < l \tag{19}$$

where σ is the index of the candidate route, $c_{v(\sigma)}^\sigma$ and c_1^σ stand for the indices of the destination and the next intersection, respectively. $rt'_{c_i^\sigma}$ represents the newly calculated time that the PEV arrives at intersection c_i^σ. $\rho^{rr}_{c_i^\sigma, c_{i+1}^\sigma}\left(\tau_{c_i^\sigma, c_{i+1}^\sigma}\right)$ denotes the updated traffic density of the real-time traffic of PEVs on the congestion-controlled road section between c_i^σ and c_{i+1}^σ, whereas $\rho^{rr,max}_{c_i^\sigma, c_{i+1}^\sigma}\left(\tau_{c_i^\sigma, c_{i+1}^\sigma}\right)$ is the maximal traffic density of the real-time traffic of PEVs allowed on the congestion-controlled road section during the future interval starting

at time $\tau_{c_i^\sigma, c_{i+1}^\sigma}$, respectively. Accordingly, if ra^σ is zero, it indicates that the lth route is not congested currently. This module then takes the route with the smallest index and checks the accessibility of the alternative route. The earlier reservation is cancelled after the alternative route is confirmed.

The step-by-step description of the algorithm is given below:

Step 1: Request for the real-time traffic condition at the end of each interval.
Step 2: Use Equations (15) through (17) to check whether the times arriving at the intersections ahead are significantly different from the original estimated times.
Step 3: Notify the metropolitan traffic monitoring center if any discrepancy exists.
Step 4: Use Equations (15) and (16) to update the arrival times of the intersections on the preferred candidate routes which were rejected during route booking.
Step 5: Check the availability of any preferred candidate route using Equations (18) and (19).
Step 6: If any preferred route is found, check with the metropolitan traffic monitoring center.
Step 7: If a preferred route is granted, take the route instead and cancel the route reservation of the original route.

3.3. Real-Time Traffic Volume Surveillance at the Metropolitan Traffic Monitoring Center

This work assumes that new incoming reservation and cancellation requests over each road section from EVs are kept in the cache. Three queues in the form of linked lists are separately maintained based on the types of the traffic flows for each road section here. They include a queue for route bookings of PEVs, that for on-road routings of PEVs, and that for EVs in rideshare fleets. At the end of the current interval, which is preset by the system operator, each cancellation request is processed first by removing the record(s) booked earlier from the corresponding linked queue. Each new request arriving at the current fixed interval is then inserted into the corresponding queue if the traffic density of the corresponding traffic flow does not reach the preset upper bound. Notably, this work allows each EV to enter the road section once it is granted during its route booking in advance. Accordingly, the traffic density of each traffic flow might exceed its preset upper bound because of the discrepancy between the arrival time at each road section predicted by SVRs and that in real time. The attributes of each queue include the identification number of the requesting EV, the time that a PEV/SAEV reaches the road section, the starting time of the fixed interval that the EV is expected to arrive at the road section, and the pointer to the next request record of the corresponding linked queue. Each queue is sorted by the arrival times of EVs.

This module first searches the linked queue based on the estimated arrival time of the PEV/SAEV, and then finds the record with the identification number of the PEV/SAEV. Now take a PEV as an example. We assume a PEV requests the cancellation of its route booking, then the record in the linked queue of route bookings is located by

$$BQ_{l,m}^{pre} \to next \to at = ev^{at} \ \& \ BQ_{l,m}^{pre} \to next \to id = ev^{id} \tag{20}$$

where ev^{at} and ev^{id} denote the estimated arrival time and the identification number of the PEV ev that requests for route cancellation during the current interval, respectively. $BQ_{l,m}^{pre}$ represents the pointer to the previous record of the booked record for ev in the route-booking queue of the PEVs on the road section between l and m. Here at and id are two attributes of the arrival time and the identification number of the PEV in the route-booking record, respectively, whereas the attribute $next$ is the pointer to the next record of the linked queue.

Then the removal of the record for the cancellation requesting PEV of the route-booking queue and the updated traffic density for the PEV's route-booking traffic flow can be expressed by

$$BQ_{l,m}^{pre} \to next = BQ_{l,m}^{pre} \to next \to next \tag{21}$$

$$\tau_{l,m} = BQ_{l,m}^{pre} \to next \to st \tag{22}$$

$$\rho_{l,m}^{rb}(\tau_{l,m}) = \max\left[\rho_{l,m}^{rb}(\tau_{l,m}) - 1, 0\right] \tag{23}$$

$$\text{delete}\left(BQ_{l,m}^{pre} \rightarrow next\right) \tag{24}$$

where *st* represents the attribute of the route-booking queue that stands for the starting time of the fixed interval that the EV reaches the section connecting *l* and *m*. $\rho_{l,m}^{rb}(\tau_{l,m})$ denotes the updated traffic density of the route-booking PEVs in a future interval starting at the time $_{l,m}$. delete($\cdot$) is the deletion function that removes the record from the linked queue. Equations (20) through (24) are iterated until all cancellation requests are removed from the route-booking queue of PEVs. Notably, the handling of cancellation requests of the on-road routing queues for the PEVs and those of rideshare bookings for autonomous EV rideshare fleets are treated likewise.

This module then determines whether a new arriving route request in each of the three queues during the current interval is allowed to drive on the section between *l* and *m*. Notably, whether an EV is a PEV or a member of autonomous EV rideshare fleet also determines the accessibility of a congestion-controlled section. The grant ratios of the three queues are adjusted dynamically during rush hours and non-rush hours. Accordingly, this module first checks how many PEVs are allowed to enter each road section by

$$\upsilon_{l,m}^{rb}(\tau_{l,m}) = \max\left[\rho_{l,m}^{rb,max}(\tau_{l,m}) - \rho_{l,m}^{rb}(\tau_{l,m}), 0\right] \tag{25}$$

$$\rho_{l,m}^{rb}(\tau_{l,m}) = \rho_{l,m}^{rb}(\tau_{l,m}) + \upsilon_{l,m}^{rb}(\tau_{l,m}) \tag{26}$$

where $\rho_{l,m}^{rb,max}(\tau_{l,m})$ denotes the maximal traffic density allowed for the route-booking PEVs within a certain future interval starting at the time $\tau_{l,m}$. $\upsilon_{l,m}^{rb}(\tau_{l,m})$ indicates the number of new route-booking PEVs granted to drive on the section between *l* and *m* in a certain future interval starting at the time $\tau_{l,m}$. Notably, the traffic density $\rho_{l,m}^{rb}(\tau_{l,m})$ remains the same if it is equal to or larger than $\rho_{l,m}^{rb,max}(\tau_{l,m})$.

In the case that $\upsilon_{l,m}^{rb}(\tau_{l,m})$ is positive, this module sorts the new route requests arriving during the current interval based on the time that the EV issued the route request. Each new granted PEV is inserted in the linked queue of route bookings by

$$BQ_{l,m}^{pre} \rightarrow at \le ev^{at} < BQ_{l,m}^{pre} \rightarrow next \rightarrow at \tag{27}$$

$$\text{new}\left(BQ_{l,m}^{new}\right) \tag{28}$$

$$BQ_{l,m}^{new} \rightarrow id = ev^{id}, \; BQ_{l,m}^{new} \rightarrow at = ev^{at}, \; BQ_{l,m}^{new} \rightarrow st = \tau_{l,m} \tag{29}$$

$$BQ_{l,m}^{pre} \rightarrow next = BQ_{l,m}^{new}, \; BQ_{l,m}^{new} \rightarrow next = BQ_{l,m}^{pre} \rightarrow next \tag{30}$$

where ev^{id} and ev^{at} denote that identification of PEV *ev* and the time that *ev* arrives at the road section, respectively. $BQ_{l,m}^{new}$ is the pointer to the newly created record of *ev* in the linked queue. Equations (27) through (30) are iterated until all granted route requests are inserted into the route-booking queue of PEVs. Meanwhile, the handling of all granted route requests of the on-road routing queues for the PEVs and those of rideshare bookings for autonomous EV rideshare fleets are treated likewise.

The step-by-step description of the algorithm is given below:

Step 1: At the end of each interval, use Equations (20) through (24) to delete the record of a new route cancellation request from the route-booking queue of PEVs at the designated road section. Step 1 is iterated until all cancellation requests are processed.

Step 2: The cancellation requests of the on-road routing queues for the PEVs and those of rideshare bookings for autonomous EV rideshare fleets are treated likewise.

Step 3: Use Equations (25) and (26) to compute the traffic density of each road section receiving new route booking request(s).

Step 4: Insert new route booking request(s) into the route-booking queue of the PEVs at the designated road section using Equations (27) through (30) if the traffic density is below a preset threshold. Steps 3 and 4 are iterated until all new route booking requests are processed.

Step 5: The route booking requests for the on-road routing queues for the PEVs and those of rideshare bookings for autonomous EV rideshare fleets are treated likewise.

3.4. Designated Rideshare Booking

As this work encourages a PEV user to book the route before departure during peak periods, the late-booking PEV user can still have a rideshare alternative if the PEV user's booking is turned down. Meanwhile, this work also assumes that the citizens living in dense, metropolitan areas find owning a vehicle to be too costly or too burdensome, and the government provide the incentive for the public to take autonomous EV rideshare fleets or public transportation for commuting.

In this work, the routes of an EV fleet member can be expressed by

$$
\mathcal{R}^\alpha = \left(\mathcal{R}_1^\alpha, \mathcal{R}_2^\alpha, \cdots, \mathcal{R}_i^\alpha, \mathcal{R}_{i+1}^\alpha, \cdots, \mathcal{R}_{p^\alpha}^\alpha \right), 1 \le \alpha \le \Phi, 1 \le i \le P^\alpha \tag{31}
$$

$$
\mathcal{R}_i^\alpha = \left[(r_{i,1}^\alpha, r_{i,2}^\alpha), (r_{i,2}^\alpha, r_{i,3}^\alpha), \cdots, \left(r_{i,fp_i^\alpha-1}^\alpha, r_{i,fp_i^\alpha}^\alpha \right), \cdots, \left(r_{i,ld_i^\alpha-1}^\alpha, r_{i,ld_i^\alpha}^\alpha \right), \cdots, \left(r_{i,cp_i^\alpha-1}^\alpha, r_{i,cp_i^\alpha}^\alpha \right) \right], \tag{32}
$$
$$
1 \le \alpha \le \Phi, 1 \le i \le P^\alpha
$$

$$
r_{i,cp_i^\alpha}^\alpha = r_{i+1,1}^\alpha, 1 \le \alpha \le \Phi, 1 \le i \le P^\alpha \tag{33}
$$

where $\mathcal{R}_i^\alpha$ represents the *i*th route of the αth SAEV fleet member. Φ is the total number of EVs operated by the designated rideshare company, whereas P^α is the number of α's rideshare routes. Notably, the sequence of α's routes also shows the schedule of rideshare routes assigned to α. $r_{i,1}^\alpha$ and $r_{i,cp_i^\alpha}^\alpha$ denote the origin and the last stop of the *i*th route assigned to fleet member α, respectively, whereas $r_{i,fp_i^\alpha}^\alpha$ and $r_{i,ld_i^\alpha}^\alpha$ represent the first pickup point and the last drop-off point on the *i*th route, respectively. Notably, both $r_{i,1}^\alpha$ and $r_{i,cp_i^\alpha}^\alpha$ are charging points that can offer charging facilities for α when its battery capacity is estimated to fall below the minimal SOC during the next rideshare route. Notably, the last node of the *i*th rideshare route $r_{i,cp_i^\alpha}^\alpha$ is also the starting node of the (*i*+1)th rideshare route $r_{i+1,1}^\alpha$ to ensure the connectivity of two consecutive rideshare routes.

Upon receiving a rideshare request, this work first checks whether a suitable rideshare service can be offered by the existing routes of the designated rideshare fleet by

$$
\underset{\alpha,i}{\arg \text{Min}} \left\{ \varpi_{i,1}^\alpha \cdot \left[\left| (x_s, y_s) - \left(x_{r_{i,pp_i^\alpha}^\alpha}, y_{r_{i,pp_i^\alpha}^\alpha} \right) \right| + \left| (x_e, y_e) - \left(x_{r_{i,dp_i^\alpha}^\alpha}, y_{r_{i,dp_i^\alpha}^\alpha} \right) \right| \right] + \varpi_{i,2}^\alpha \cdot \left(rt_{r_{i,dp_i^\alpha}^\alpha} - pt_{r_{i,pp_i^\alpha}^\alpha} \right) \right\},
$$
$$
1 \le \alpha \le \Phi, 1 \le i \le P^\alpha, 1 \le pp_i^\alpha < dp_i^\alpha \le cp_i^\alpha \tag{34}
$$

subject to:

$$
\left| (x_s, y_s) - \left(x_{r_{i,pp_i^\alpha}^\alpha}, y_{r_{i,pp_i^\alpha}^\alpha} \right) \right| \le \delta^d, 1 \le \alpha \le \Phi, 1 \le i \le P^\alpha, 1 \le pp_i^\alpha < cp_i^\alpha \tag{35}
$$

$$
\left| (x_e, y_e) - \left(x_{r_{i,dp_i^\alpha}^\alpha}, y_{r_{i,dp_i^\alpha}^\alpha} \right) \right| \le \delta^d, 1 \le \alpha \le \Phi, 1 \le i \le P^\alpha, 1 \le dp_i^\alpha \le cp_i^\alpha \tag{36}
$$

$$
0 \le rt_{r_{i,pp_i^\alpha}^\alpha} - pt_{r_{i,pp_i^\alpha}^\alpha} \le \delta^t, 1 \le \alpha \le \Phi, 1 \le i \le P^\alpha, 1 \le pp_i^\alpha < cp_i^\alpha \tag{37}
$$

$$
pn_{r_{i,pp_i^\alpha}^\alpha}^{cur} + pn_{r_{i,pp_i^\alpha}^\alpha}^{new} \le pn^{\alpha,max}, 1 \le \alpha \le \Phi, 1 \le i \le P^\alpha, 1 \le pp_i^\alpha < cp_i^\alpha \tag{38}
$$

where $\varpi_{i,1}^{\alpha}$ and $\varpi_{i,2}^{\alpha}$ represent the two weights of the rideshare passenger's optimization objectives. (x_s, y_s) and (x_e, y_e) denote the rideshare passenger's departure and the destination locations, respectively. Here, two intersections $r_{i,pp_i^{\alpha}}^{\alpha}$ and $r_{i,dp_i^{\alpha}}^{\alpha}$ are designated as the pickup and the drop-off point, and $\left(x_{r_{i,pp_i^{\alpha}}^{\alpha}}, y_{r_{i,pp_i^{\alpha}}^{\alpha}}\right)$ and $\left(x_{r_{i,dp}^{\alpha}}, y_{r_{i,dp}^{\alpha}}\right)$ are the corresponding coordinates, respectively. $rt_{r_{i,pp_i^{\alpha}}^{\alpha}}$ and $pt_{r_{i,pp_i^{\alpha}}^{\alpha}}$ denote the arrival time for and that for the rideshare passenger to arrive at $r_{i,pp_i^{\alpha}}^{\alpha}$, respectively. δ^d and δ^t represent the maximal time that the passenger can wait at the pickup point and the maximal distance for the passenger to reach the pickup/drop-off point, respectively. $pn_{r_{i,pp_i^{\alpha}}^{\alpha}}^{cur}$ is the number of the riders on SAEV α before it reaches $r_{i,pp_i^{\alpha}}^{\alpha}$, $pn_{r_{i,pp_i^{\alpha}}^{\alpha}}^{new}$ is the number of passenger(s) α picks up at $r_{i,pp_i^{\alpha}}^{\alpha}$, whereas $pn^{\alpha,max}$ denote α's maximal seating capacity. Accordingly, the value of $pn_{r_{i,pp_i^{\alpha}}^{\alpha}}^{cur}$ is set to $pn_{r_{i,pp_i^{\alpha}}^{\alpha}}^{cur} + pn_{r_{i,pp_i^{\alpha}}^{\alpha}}^{new}$ if $pn_{r_{i,pp_i^{\alpha}}^{\alpha}}^{new}$ new passenger(s) is pickup up at $r_{i,pp_i^{\alpha}}^{\alpha}$.

The first optimization objective in Equation (34) stands for the distance between the rideshare requesting passenger's origin and the pickup point plus the distance between the requester's drop-off location and her/his destination. The second objective indicates the time that the requester waits at the pickup point until SAEV α arrives. The weight of each optimization objective is the priority of the corresponding objective. Here the routes of all fleet members are examined, and the most suitable route is calculated from the two optimized target values in Equation (34) based on the constraints of Equations (35) through (38).

If the fleet cannot assign a member to serve the requester, this work in turn attempts to extend one of the rideshare routes of some SAEV or creates a new route for a SAEV which is currently off duty by

$$
\begin{aligned}
\underset{\alpha,i}{\arg\,\mathrm{Min}} & \left\{ \varpi_{i,1}^{\alpha} \cdot \left[\left| (x_s, y_s) - \left(x_{r_{i,pp_i^{\alpha}}^{\alpha}}, y_{r_{i,pp_i^{\alpha}}^{\alpha}}\right) \right| + \left| (x_e, y_e) - \left(x_{r_{i,dp_i^{\alpha}}^{\alpha}}, y_{r_{i,dp_i^{\alpha}}^{\alpha}}\right) \right| \right] + \varpi_{i,2}^{\alpha} \cdot \left(rt_{r_{i,dp_i^{\alpha}}^{\alpha}} - pt_{r_{i,pp_i^{\alpha}}^{\alpha}} \right) + \varpi_{i,3}^{\alpha} \cdot \right. \\
& \left. \left[\phi_{r_{i,1}^{\alpha}} \cdot RP_{r_{i,1}^{\alpha}}\left(rt_{r_{i,1}^{\alpha}}\right) \cdot pcp_{r_{i,1}^{\alpha}} \cdot ct_{r_{i,1}^{\alpha}} + \theta_{r_{i,j}^{\alpha}, r_{i,j+1}^{\alpha}} \cdot WP_{r_{i,j}^{\alpha}, r_{i,j+1}^{\alpha}}\left(rt_{r_{i,j}^{\alpha}}\right) \cdot wcp_{r_{i,j}^{\alpha}, r_{i,j+1}^{\alpha}} \cdot SD_{r_{i,j}^{\alpha}, r_{i,j+1}^{\alpha}}\left(rt_{r_{i,j}^{\alpha}}\right) + \Psi_{r_{i,1}^{\alpha}} \cdot \right. \\
& \left. \left. RP_{r_{i,1}^{\alpha}}\left(rt_{r_{i,1}^{\alpha}}\right) \cdot \left[SOC^{\alpha,max} - SOC_{r_{i,1}^{\alpha}}^{\alpha} \right] \right] \right\}, \ 1 \leq \alpha \leq \Phi, 1 \leq i \leq \mathrm{P}^{\alpha}
\end{aligned} \tag{39}
$$

subject to

$$
\mathcal{R}_i^{\alpha} = \left[(r_{i,1}^{\alpha}, r_{i,2}^{\alpha}), \cdots, \left(r_{i,fp_i^{\alpha}-1}^{\alpha}, r_{i,fp_i}^{\alpha}\right), \cdots, \left(r_{i,ld_i^{\alpha}-1}^{\alpha}, r_{i,ld_i}^{\alpha}\right), \cdots, \left(r_{i,pp_i^{\alpha}-1}^{\alpha}, r_{i,pp_i^{\alpha}}^{\alpha}\right), \cdots, \right. \tag{40}
$$

$$
\left. \left(r_{i,dp_i^{\alpha}-1}^{\alpha}, r_{i,dp_i^{\alpha}}^{\alpha}\right), \cdots, \left(r_{i,cp_i^{new}-1}^{\alpha}, r_{i,cp_i^{new}}^{\alpha}\right) \right], 1 \leq \alpha \leq \Phi, 1 \leq i \leq p^{\alpha}
$$

$$
\mathcal{R}_{i+1}^{\alpha} = \left[(r_{i+1,1^{new}}^{\alpha}, r_{i+1,2^{new}}^{\alpha}), \cdots, \left(r_{i+1,fp_{i+1}^{\alpha}}^{\alpha}, r_{i+1,fp_{i+1}}^{\alpha}\right), \cdots, \left(r_{i+1,ld_{i+1}^{\alpha}-1}^{\alpha}, r_{i+1,ld_{i+1}}^{\alpha}\right), \right. \tag{41}
$$

$$
\left. \cdots, \left(r_{i+1,cp_{i+1}^{\alpha}-1}^{\alpha}, r_{i+1,cp_{i+1}}^{\alpha}\right) \right], 1 \leq \alpha \leq \Phi, \ 1 \leq i < \mathrm{P}^{\alpha}
$$

$$
r_{i+1,1^{new}}^{\alpha} = r_{i,cp_i^{\alpha,new}}^{\alpha}, \ 1 \leq \alpha \leq \Phi, 1 \leq i < \mathrm{P}^{\alpha} \tag{42}
$$

$$
\begin{aligned}
rt_{r_{i,j+1}^{\alpha}} = rt_{r_{i,j}^{\alpha}} + \kappa_{r_{i,j}^{\alpha}} \cdot PD_{r_{i,j}^{\alpha}, r_{i,j+1}^{\alpha}}\left(pn_{r_{i,j}^{\alpha}}^{new}\right) + ID_{r_{i,j}^{\alpha}, r_{i,j+1}^{\alpha}}\left(rt_{r_{i,j}^{\alpha}}\right) + SD_{r_{i,j}^{\alpha}, r_{i,j+1}^{\alpha}}\left(rt_{r_{i,j}^{\alpha}}\right), \\
1 \leq \alpha \leq \Phi, \ 1 \leq i \leq \mathrm{P}^{\alpha}, 1 \leq j < r_{i,cp_i^{\alpha,new}}^{\alpha}
\end{aligned} \tag{43}
$$

$$
\begin{aligned}
SoC_{r_{i,j+1}^{\alpha}} = SoC_{r_{i,j}^{\alpha}} & + \eta^{\alpha} \cdot \theta_{r_{i,j}^{\alpha}, r_{i,j+1}^{\alpha}} \cdot wcp_{r_{i,j}^{\alpha}, r_{i,j+1}^{\alpha}} \cdot SD_{r_{i,j}^{\alpha}, r_{i,j+1}^{\alpha}}\left(rt_{r_{i,j}^{\alpha}}\right) + \eta^{\alpha} \cdot \phi_{r_{i,j}^{\alpha}} \cdot pcp_{c_i^l} \cdot ct_{r_{i,j}^{\alpha}} + \Psi_{r_{i,j}^{\alpha}} \\
& \cdot \left(SOC^{\alpha,max} - SoC_{r_{i,j}^{\alpha}} \right) - ap \cdot sl_{r_{i,j}^{\alpha}, r_{i,j+1}^{\alpha}}, \ 1 \leq \alpha \leq \Phi, 1 \leq i \leq \mathrm{P}^{\alpha}, 1 \leq j < r_{i,cp_i^{\alpha,new}}^{\alpha}
\end{aligned} \tag{44}
$$

$$
pt_{r_{i,pp_i^{\alpha}}^{\alpha}} \leq rt_{r_{i,pp_i^{\alpha}}^{\alpha}}, \ 1 \leq \alpha \leq \Phi, \ 1 \leq i \leq \mathrm{P}^{\alpha} \tag{45}
$$

$$rt_{r^\alpha_{i,cp^\alpha_i,new}} + \phi_{r^\alpha_{i,cp^\alpha_i,new}} \cdot ct_{r^\alpha_{i,cp^\alpha_i,new}} + \Psi_{r^\alpha_{i,cp^\alpha_i,new}} \cdot BSD_{r^\alpha_{i,cp^\alpha_i,new}}\left(rt_{r^\alpha_{i,cp^\alpha_i,new}}\right) \le dt_{r^\alpha_{i+1,1^{new}}}, \quad 1 \le \alpha \le \Phi, \ 1 \le i < p^\alpha \tag{46}$$

$$pn^{cur}_{r^\alpha_{i,pp^\alpha_i}} + pn^{new}_{r^\alpha_{i,pp^\alpha_i}} \le pn^{\alpha,max}, \ 1 \le \alpha \le \Phi, 1 \le i \le \mathrm{P}^\alpha \tag{47}$$

$$\rho^{rf}_{r^\alpha_{i,j},r^\alpha_{i,j+1}}\left(\tau_{r^\alpha_{i,j},r^\alpha_{i,j+1}}\right) < \rho^{rf,max}_{r^\alpha_{i,j},r^\alpha_{i,j+1}}\left(rt_{r^\alpha_{i,j}}\right), \tag{48}$$

$$\tau_{r^\alpha_{i,j},r^\alpha_{i,j+1}} \le rt_{r^\alpha_{i,j}} <_{r^\alpha_{i,j},r^\alpha_{i,j+1}} +\Delta, \ 1 \le \alpha \le \Phi, 1 \le i \le \mathrm{P}^\alpha, 1 \le j < r^\alpha_{i,cp^\alpha_i,new}$$

$$0 \le ct_{r^\alpha_{i,1}} \le ct^{max}_{r^\alpha_{i,1}}, \ \text{if } \phi_{r^\alpha_{i,1}} = 1 \tag{49}$$

$$SOC^{\alpha,min} \le SoC_{r^\alpha_{i,j}} \le SOC^{\alpha,max}, \ 1 \le i \le p^\alpha, 1 \le j \le r^\alpha_{i,cp^\alpha_i,new} \tag{50}$$

$$\sum_{\substack{1 \le i \le p^\alpha \\ 1 \le j < r^\alpha_{i,cp^\alpha_i,new}}} \left(\phi_{r^\alpha_{i,1}} + \theta_{r^\alpha_{i,j},r^\alpha_{i,j+1}} + \Psi_{r^\alpha_{i,1}}\right) \ge 1, \tag{51}$$

$$\text{if } SOC^\alpha_{r^\alpha_{i,1}} - ap^\alpha \cdot \sum_{1 \le j < r^\alpha_{i,cp^\alpha_i,new}} sl_{r^\alpha_{i,j},r^\alpha_{i,j+1}} < SOC^{\alpha,min}$$

$$0 \le \eta^\alpha \le 1 \tag{52}$$

The parameters adopted in the equations shown above are defined as follows:

- $\varpi^\alpha_{i,1}$, $\varpi^\alpha_{i,2}$ and $\varpi^\alpha_{i,3}$ denote the three weights of the fleet's optimization objectives. $\mathcal{R}^\alpha_i$ and $\mathcal{R}^\alpha_{i+1}$ represent the ith and $(i+1)$th rideshare routes of SAEV α after accepting the new assignment of serving the rideshare requester(s).
- r^α_{i,fp^α} and r^α_{i,ld^α_i} stand for the first pickup and the last drop-off points of α's ith rideshare route before serving the new rideshare requester, respectively, whereas r^α_{i,pp^α} and r^α_{i,dp^α} are the new rideshare requester's pickup and drop-off locations, respectively. $r^\alpha_{i,cp^\alpha_i,new}$ represents the charging point at the end of the extended ith rideshare route. $r^\alpha_{i+1,1^{new}}$ and $r^\alpha_{i+1,2^{new}}$ denote the new starting node and the second intersection on α's updated $(i+1)$th route. Notably, $r^\alpha_{i+1,1^{new}}$ is identical to $r^\alpha_{i,cp^\alpha_i,new}$ to ensure the connectivity of the ith and $(i+1)$th rideshare routes.
- $SD_{r^\alpha_{i,j},r^\alpha_{i,j+1}}(t)$ denotes the time SAEV α passes through the section connecting $r^\alpha_{i,j}$ and $r^\alpha_{i,j+1}$ at time t. $ID_{r^\alpha_{i,j},r^\alpha_{i,j+1}}(t)$ stands for the time α stays at the intersection $r^\alpha_{i,j}$ at time t. $\kappa_{r^\alpha_{i,j}}$ is a binary flag indicating if $r^\alpha_{i,j}$ is the pickup/drop off point. $PD_{r^\alpha_{i,j},r^\alpha_{i,j+1}}\left(pn^{new}_{r^\alpha_{i,j}}\right)$ is the estimated time that the rideshare passenger $pn^{new}_{r^\alpha_{i,j}}$ waits at $r^\alpha_{i,j}$. $pn^{cur}_{r^\alpha_{i,pp^\alpha}}$ represents the number of the riders that α carries when it reaches r^α_{i,pp^α}, $pn^{new}_{r^\alpha_{i,pp^\alpha}}$ is the number of rideshare requester(s) pickup up at r^α_{i,pp^α}, whereas $pn^{\alpha,max}$ is α's maximal seating capacity. Notably, the value of $pn^{cur}_{r^\alpha_{i,pp^\alpha}}$ will be set to $pn^{cur}_{r^\alpha_{i,pp^\alpha}} + pn^{new}_{r^\alpha_{i,pp^\alpha}}$ after α picks up $pn^{new}_{r^\alpha_{i,pp^\alpha}}$ new passengers at r^α_{i,pp^α}. In addition, the values of $SD_{r^\alpha_{i,j},r^\alpha_{i,j+1}}(\cdot)$, $ID_{r^\alpha_{i,j},r^\alpha_{i,j+1}}(\cdot)$ and $PD_{r^\alpha_{i,j},r^\alpha_{i,j+1}}(\cdot)$ are also estimated with SVRs.
- $RP_{r^\alpha_{i,1}}\left(rt_{r^\alpha_{i,1}}\right)$ denotes the charging cost of the plug & charge or battery exchange service indexed by $r^\alpha_{i,1}$ at time $rt_{r^\alpha_{i,1}}$, whereas $WP_{r^\alpha_{i,j},r^\alpha_{i,j+1}}\left(rt_{r^\alpha_{i,j}}\right)$ denotes that of electric road charging over the section between $r^\alpha_{i,j}$ and $r^\alpha_{i,j+1}$ at time $rt_{r^\alpha_{i,j}}$. $pcp_{r^\alpha_{i,1}}$ and $wcp_{r^\alpha_{i,j},r^\alpha_{i,j+1}}$ denote the charging power/second for the plug & charge station indexed by $r^\alpha_{i,1}$ and that for the electric road charging over the section connecting $r^\alpha_{i,j}$ and $r^\alpha_{i,j+1}$, respectively. $ct_{r^\alpha_{i,1}}$ is the time that the fleet member gets charged and $ct^{max}_{r^\alpha_{i,1}}$ is the maximal

time that the fleet member is allowed to be charged at the plug and charge station $r_{i,1}^\alpha$, respectively.

- $sl_{r_{i,j}^\alpha, r_{i,j+1}^\alpha}$ stands for the road length between $r_{i,j}^\alpha$ and $r_{i,j+1}^\alpha$. $rt_{r_{i,pp_i}^\alpha}^\alpha$ and $pt_{r_{i,pp_i}^\alpha}^\alpha$ denote the arrival time for SAEV α and that for the rideshare passenger to arrive at r_{i,pp_i}^α, respectively, whereas $dt_{r_{i+1,1^{new}}^\alpha}$ stands for α's departure time of the updated $(i+1)$th route. Notably, The departure time for the $(i+1)$th route should be later than the time that α arrives at charging point, $r_{i+1,1^{new}}^\alpha$, plus the battery charging time of α.

- $SOC^{\alpha,max}$ and $SOC^{\alpha,min}$ stand for the maximal and the minimal battery capacity of SAEV α, respectively, whereas $SOC_{r_{i,1}^\alpha}^\alpha$ denotes α's battery capacity when it reaches $r_{i,1}^\alpha$. The binary flags $\phi_{r_{i,1}^\alpha}$ and $\Psi_{r_{i,1}^\alpha}$ are used to mark whether a plug & charge station and a battery exchange service located at $r_{i,1}^\alpha$ is chosen for recharging, respectively. $\theta_{r_{i,j}^\alpha, r_{i,j+1}^\alpha}$ is used to indicate if electric road charging that connects $r_{i,j}^\alpha$ and $r_{i,j+1}^\alpha$ is used to charge α's battery. ap^α is the power consumption of α's battery per kilometer, whereas η^α denotes the charging efficiency of α's battery.

- $\rho_{r_{i,j}^\alpha, r_{i,j+1}^\alpha}^{rf}\left(\tau_{r_{i,j}^\alpha, r_{i,j+1}^\alpha}\right)$ and $\rho_{r_{i,j}^\alpha, r_{i,j+1}^\alpha}^{rf,max}\left(rt_{r_{i,j}^\alpha}\right)$ denote that the current and the maximal traffic flow for the fleet during the future interval starting at time $\tau_{r_{i,j}^\alpha, r_{i,j+1}^\alpha}$, respectively.

The first optimization objective in Equation (39) is used to measure the distance between the rideshare requester's departure location and the pickup point plus the length measured from the requester's drop-off location to her/his destination. The second objective denotes the travelling time of SAEV α that the requester spends on the ride, and the third objective stands for the charging cost of α's ith route. The routes of all fleet members are examined, and the most suitable route is calculated from the three optimized target values in Equation (39) based on the constraints of Equations (40) through (52). In the event that no qualified rideshare route is available, the rideshare company will send the rideshare request to the coordinator to check if a route offered by any other service provider is qualified for the requester's demand.

The step-by-step description of the algorithm is given below:

Step 1: Upon receiving a rideshare request, use Equations (34) through (38) to check whether a suitable rideshare service can be offered by the existing routes of the designated rideshare fleet.

Step 2: If no existing rideshare routes are found, use Equations (39) through (52) to extend the rideshare route of some fleet member or create a new route for a SAEV which is off duty.

Step 3: If no qualified rideshare route is available, notify the coordinator to check whether any other rideshare service provider can satisfy the rideshare request.

3.5. Real Time Rideshare Coordination

This work assumes all rideshare companies regularly submit the rideshare routes of their SAEV fleets to the rideshare coordinator at regular intervals, and then the coordinator updates the database at its cache accordingly. Upon receiving a request from a rideshare company that needs the support of any other rideshare company to offer the rideshare service for a requester, the rideshare coordinator checks with the database if any suitable candidate rideshare service is available. The rideshare company that offers the candidate rideshare service will then be asked by the coordinator to confirm that the new rideshare request can be fit into the rideshare route. The coordinator will notify the requester if the assigned rideshare company acknowledges the request. Otherwise, it implies the SAEVs of all rideshare companies are fully booked. The requester will be suggested to take public transportation instead.

The rideshare routes kept in the cache of the rideshare coordinator can be expressed by

$$\mathcal{R}^{k,\alpha} = \left(\mathcal{R}_1^{k,\alpha}, \mathcal{R}_2^{k,\alpha}, \cdots, \mathcal{R}_i^{k,\alpha}, \mathcal{R}_{i+1}^{k,\alpha}, \cdots, \mathcal{R}_{p^{k,\alpha}}^{k,\alpha}\right), \ 1 \le k \le \Theta, 1 \le \alpha \le \Phi^k, 1 \le i \le P^{k,\alpha} \tag{53}$$

$$\mathcal{R}_i^{k,\alpha} = \left[\left(r_{i,1}^{k,\alpha}, r_{i,2}^{k,\alpha} \right), \left(r_{i,2}^{k,\alpha}, r_{i,3}^{k,\alpha} \right), \cdots, \left(r_{i,fp_i^{k,\alpha}-1}^{k,\alpha}, r_{i,fp_i^{k,\alpha}}^{k,\alpha} \right), \cdots, \left(r_{i,ld_i^{k,\alpha}-1}^{k,\alpha}, r_{i,ld_i^{k,\alpha}}^{k,\alpha} \right), \right. \tag{54}$$

$$\left. \cdots, \left(r_{i,cp_i^{k,\alpha}-1}^{k,\alpha}, r_{i,cp_i^{k,\alpha}}^{k,\alpha} \right) \right], 1 \le k \le \Theta, 1 \le \alpha \le \Phi^k, 1 \le i \le^{k,\alpha}$$

$$r_{i,cp_i^{k,\alpha}}^{k,\alpha} = r_{i+1,1}^{k,\alpha}, \ 1 \le k \le \Theta, 1 \le \alpha \le \Phi^k, 1 \le i \le^{k,\alpha} \tag{55}$$

where $\mathcal{R}_i^{k,\alpha}$ stands for the ith route of SAEV α operated by the rideshare company indexed by k.θ denotes the number of rideshare companies, Φ^k is the total number of EVs operated by the rideshare company k, whereas $P^{k,\alpha}$ is the number of α's rideshare routes assigned by rideshare company k. $r_{i,1}^{k,\alpha}$ and $r_{i,cp_i^{k,\alpha}}^{k,\alpha}$ denote the origin and the last stop of the ith route assigned to α, respectively; whereas $r_{i,fp_i^{k,\alpha}}^{k,\alpha}$ and $r_{i,ld_i^{k,\alpha}}^{k,\alpha}$ represent the first pickup point and the last drop-off point on the ith route of α, respectively.

Based on the updated database at its cache, rideshare coordinator first checks whether a suitable rideshare service can be offered by the existing routes of the rideshare fleet operated by the service provider indexed by k:

$$\underset{\alpha,i}{\arg\text{Min}} \left\{ \omega_{i,1}^{k,\alpha} \cdot \left[\left| (x_s, y_s) - \left(x_{r_{i,pp_i^{k,\alpha}}^{k,\alpha}}, y_{r_{i,pp_i^{k,\alpha}}^{k,\alpha}} \right) \right| + \left| (x_e, y_e) - \left(x_{r_{i,dp_i^{k,\alpha}}^{k,\alpha}}, y_{r_{i,dp_i^{k,\alpha}}^{k,\alpha}} \right) \right| \right] + \omega_{i,2}^{k,\alpha} \cdot \left(rt_{r_{i,dp_i^{k,\alpha}}^{k,\alpha}} - pt_{r_{i,pp_i^{k,\alpha}}^{k,\alpha}} \right) \right\}, \tag{56}$$
$$1 \le k \le \Theta, 1 \le \alpha \le \Phi^k, 1 \le i \le P^{k,\alpha}, \ 1 \le pp_i^{k,\alpha} < dp_i^{k,\alpha} \le cp_i^{k,\alpha}$$

subject to

$$\left| (x_s, y_s) - \left(x_{r_{i,pp_i^{k,\alpha}}^{\alpha}}, y_{r_{i,pp_i^{k,\alpha}}^{\alpha}} \right) \right| \le \delta^d, \tag{57}$$

$$1 \le k \le \Theta, 1 \le \alpha \le \Phi^k, 1 \le i \le P^{k,\alpha}, 1 \le pp_i^{k,\alpha} < cp_i^{k,\alpha}$$

$$\left| (x_e, y_e) - \left(x_{r_{i,dp_i^{k,\alpha}}^{k,\alpha}}, y_{r_{i,dp_i^{k,\alpha}}^{k,\alpha}} \right) \right| \le \delta^d, \tag{58}$$

$$1 \le k \le \Theta, 1 \le \alpha \le \Phi^k, 1 \le i \le P^{k,\alpha}, 1 \le dp_i^{k,\alpha} \le cp_i^{k,\alpha}$$

$$0 \le rt_{r_{i,pp_i^{k,\alpha}}^{k,\alpha}} - pt_{r_{i,pp_i^{k,\alpha}}^{k,\alpha}} \le \delta^t, 1 \le k \le \Theta, 1 \le \alpha \le \Phi^k, 1 \le i \le P^{k,\alpha}, \ 1 \le pp_i^{k,\alpha} < cp_i^{k,\alpha} \tag{59}$$

$$pn_{r_{i,pp_i^{k,\alpha}}^{k,\alpha}}^{cur} + pn_{r_{i,pp_i^{k,\alpha}}^{k,\alpha}}^{new} \le pn^{k,\alpha,max}, \tag{60}$$

$$1 \le k \le \Theta, 1 \le \alpha \le \Phi^k, 1 \le i \le P^{k,\alpha}, \ 1 \le pp_i^{k,\alpha} < cp_i^{k,\alpha}$$

where α denotes the index of the SAEV, and SAEV α is a fleet member of rideshare company indexed by k. $\omega_{i,1}^{k,\alpha}$ and $\omega_{i,2}^{k,\alpha}$ represent the two weights of the rideshare passenger's optimization objectives. $r_{i,pp_i^{k,\alpha}}^{k,\alpha}$ and $r_{i,dp_i^{k,\alpha}}^{k,\alpha}$ stand for the pickup and the drop-off point, respectively. $\left(x_{r_{i,pp_i^{k,\alpha}}^{k,\alpha}}, y_{r_{i,pp_i^{k,\alpha}}^{k,\alpha}} \right)$ represents the location of the pickup point, and $\left(x_{r_{i,dp_i^{k,\alpha}}^{k,\alpha}}, y_{r_{i,dp_i^{k,\alpha}}^{k,\alpha}} \right)$ is that of drop-off point, respectively. $rt_{r_{i,pp_i^{k,\alpha}}^{k,\alpha}}$ and $pt_{r_{i,pp_i^{k,\alpha}}^{k,\alpha}}$ stand for the arrival time for SAEV α and that for the rideshare passenger to arrive at $r_{i,pp_i^{k,\alpha}}^{k,\alpha}$, respectively. $pn_{r_{i,pp_i^{k,\alpha}}^{k,\alpha}}^{cur}$, $pn_{r_{i,pp_i^{k,\alpha}}^{k,\alpha}}^{new}$ and $pn^{k,\alpha,max}$ are the number of the passengers that SAEV α carries after it reaches $r_{i,pp_i^{k,\alpha}}^{k,\alpha}$, the number of rideshare requester(s) picked up at $r_{i,pp_i^{k,\alpha}}^{k,\alpha}$, and the maximal

seating capacity of α, respectively. The value of $pn^{cur}_{r^{k,\alpha}_{i,pp^{k,\alpha}_i}}$ is set to $pn^{cur}_{r^{k,\alpha}_{i,pp^{k,\alpha}_i}} + pn^{new}_{r^{k,\alpha}_{i,pp^{k,\alpha}_i}}$ if α

picks up $pn^{new}_{r^{k,\alpha}_{i,pp^{k,\alpha}_i}}$ new passenger(s) at $r^{k,\alpha}_{i,pp^{k,\alpha}_i}$.

The first optimization objective in Equation (56) stands for the distance between the rideshare requesting passenger's origin and the pickup point plus the distance between the requester's drop-off location and her/his destination. The second objective indicates the time that the requester waits at the pickup point until SAEV α owned by rideshare company k arrives. The priority of each objective is reflected by the weight set for the corresponding objective. The routes of all fleets maintained by the rideshare coordinator are examined, and the most suitable route is calculated from the two optimized target values in Equation (56) based on the constraints of Equations (57) through (60).

If no suitable rideshare service can be offered by the existing routes operated by all rideshare companies, the coordinator will look for the candidates that can extend from their current route plans. The cache is checked again to pick up all candidate route with the time that the requester arrives at the pickup point falling between the time that SAEV α leaves the last drop-off point of a route and that of the first pickup point of its next route. That is,

$$rt_{r^{k,\alpha}_{i,ld^{k,\alpha}_i}} < pt_{r^{k,\alpha}_{i,pp^{k,\alpha}_i}} < rt_{r^{k,\alpha}_{i+1,fp^{k,\alpha}_{i+1}}}, 1 \leq k \leq \Theta, 1 \leq \alpha \leq \Phi^k, 1 \leq i < P^{k,\alpha} \qquad (61)$$

Next, the chosen candidate routes are sorted in ascending order according to the value of $rt_{r^{k,\alpha}_{i+1,fp^{k,\alpha}_{i+1}}} - rt_{r^{k,\alpha}_{i,ld^{k,\alpha}_i}}$. Starting from the first element of the sorted list, the coordinator notifies the rideshare company that operates the selected route to check if the candidate route can be extended to cope with the requester's demand. Notably, the algorithm given in Section 3.1 can be applied to compute the time the SAEV driving from $rt_{r^{k,\alpha}_{i,ld^{k,\alpha}_i}}$ to the pickup point of the requester, the time that the requester takes the ride, and the time the SAEV driving from the drop-off point to $rt_{r^{k,\alpha}_{i+1,fp^{k,\alpha}_{i+1}}}$.

Once a rideshare route is available, the requester and the coordinator will be informed by the rideshare route operator. Otherwise, the coordinator will notify the next service provider on the list. In the case that no candidates qualify the requester's demand, the requester will receive a scheduled public transport for reference.

The step-by-step description of the algorithm is given below:

Step 1: Upon receiving a rideshare matching request, use Equations (56) through (60) to check whether the rideshare service can be offered by the existing routes of some rideshare fleet.

Step 2: If no existing rideshare routes are found, use Equation (61) to obtain the list of all candidate SAEVs that can possible extend the rideshare service from their route plans.

Step 3: Sort the route in ascending order according to the value of $rt_{r^{k,\alpha}_{i+1,fp^{k,\alpha}_{i+1}}} - rt_{r^{k,\alpha}_{i,ld^{k,\alpha}_i}}$.

Step 4: Starting form the first element of the sorted list, apply the algorithm given in Section 3.1 to compute the time the SAEV driving from $rt_{r^{k,\alpha}_{i,ld^{k,\alpha}_i}}$ to the pickup point of the requester, the time that the requester takes the ride, and the time the SAEV driving from the drop-off point to $rt_{r^{k,\alpha}_{i+1,fp^{k,\alpha}_{i+1}}}$. This step is iterated until all elements of the sorted list are checked, or a qualified rideshare route is found.

Step 5: Check if $rt_{r^{k,\alpha}_{i+1,fp^{k,\alpha}_{i+1}}} - rt_{r^{k,\alpha}_{i,ld^{k,\alpha}_i}}$ is larger than the total time for the SAEV driving from $rt_{r^{k,\alpha}_{i,ld^{k,\alpha}_i}}$ to $rt_{r^{k,\alpha}_{i+1,fp^{k,\alpha}_{i+1}}}$ as computed at Step 4. If no qualified rideshare route is found,

iterate Steps 4 and 5 until all elements of the sorted list are checked, or a qualified rideshare route is found.

Step 6: If no qualified rideshare route is available, inform the requester of a scheduled public transport for reference.

4. Experimental Results and Analysis

The feasibility and effectiveness of the proposed mechanism was evaluated through four different scenarios in the simulation with a personal computer (I5-10400/2.90 GHz CPU/16 GB RAM), and the Python programming language was adopted to implement the proposed work described above. The traffic data were collected and extended from a traffic condition website in Taiwan [39]. The total number of the records collected from the traffic dataset is 17,280. The components of the traffic dataset include the average driving speed of a vehicle and traffic flow measured at the intersections every five minutes. The road section observed consists of one six-lane major arterial road, two four-lane minor arterial roads and 21 local municipal roads as shown in Table 2, and the corresponding road network of the selected urban area is shown in Figure 2. The two minor arterial roads are parallel to the major arterial road. The major arterial road offers electric road charging in order to allow a PEV/SAEV to charge its battery during driving. One battery exchange service is located at the intersection of each minor arterial road, and the battery exchange time is 3 min [40]. Six plug and charge stations are separately deployed at the intersections of municipal roads. All route requests of EV users were randomly generated, and the pickup and the drop-off location of each passenger was generated with uniform distribution. The time that an EV stops at an intersection for pickup and drop-off was set within 15 seconds, whereas the delay of a PEV/SAEV waits at an intersection due to traffic light control was set randomly within 1 minute. The traffic density allowed on the major and minor arterial roads was limited to 50 EVs per km [41].

**Table 2.** The 24 different road sections used in the simulation.

Road Type	Road Name	Road Type	Road Name
Major arterial road	Huanzhong Road	Local municipal road	Yongchun East Road
Minor arterial 1	Liming Road	Local municipal road	Jingcheng Road
Minor arterial 2	Zhongqing Road	Local municipal road	Nantun Road
Local municipal road	Chongde Road	Local municipal road	Yingcai Road
Local municipal road	Songzhu Road	Local municipal road	Taiyuan Road
Local municipal road	Zhongke Road	Local municipal road	Wenxin Road
Local municipal road	Kaixuan Road	Local municipal road	Dunhua Road
Local municipal road	Xitun Road	Local municipal road	Dalian Road
Local municipal road	Taiwan Blvd	Local municipal road	Shanxi Road
Local municipal road	Shizheng Road	Local municipal road	Houzhuang Road
Local municipal road	Gongyi Road	Local municipal road	Siping Road
Local municipal road	Wuquan West Road	Local municipal road	Henan Road

Figure 3 shows the original traffic volumes on all the road sections before running the proposed algorithm. Notably, no rideshare services are provided at the original scenario of the simulation. That is, it was assumed only PEVs drove on all road sections in the original scenario. Since the two minor arterial roads are parallel to the major arterial road, most of PEV drivers with longer travel distances took the major arterial road as the preferred routes to their destinations, not to mention the PEV drivers with urgent charging demand owing to the offering of electric road charging on the major arterial road. Meanwhile, each resident living at the surrounding area of the two minor arterial roads takes her/his nearby minor arterial road for commuting. Accordingly, it can be seen from Figure 3 that serious traffic jams occurred on the major arterial road during rush hours in a day. Conversely, the observed traffic volumes on the two minor arterial roads and municipal roads are significantly smaller than that of the major arterial road.
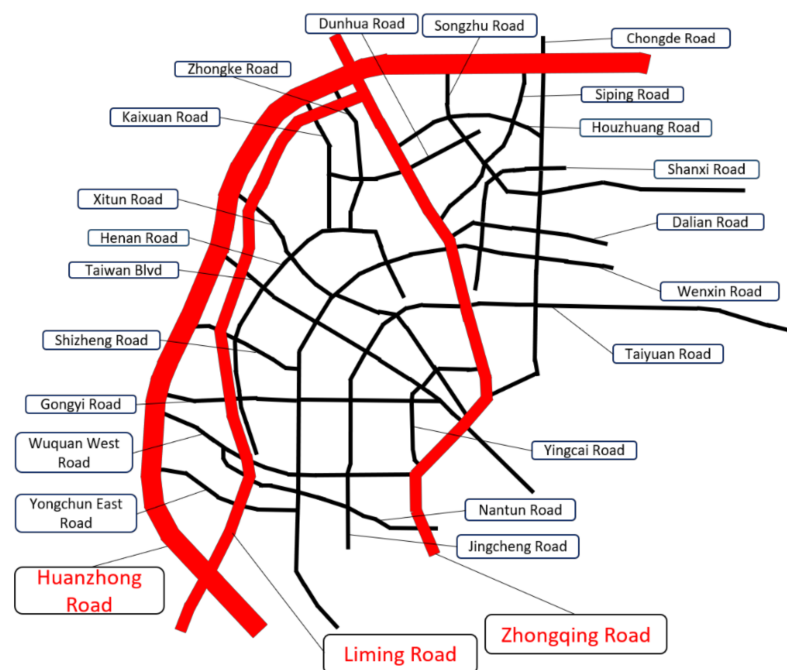
Figure 2. Road network of the selected urban area.
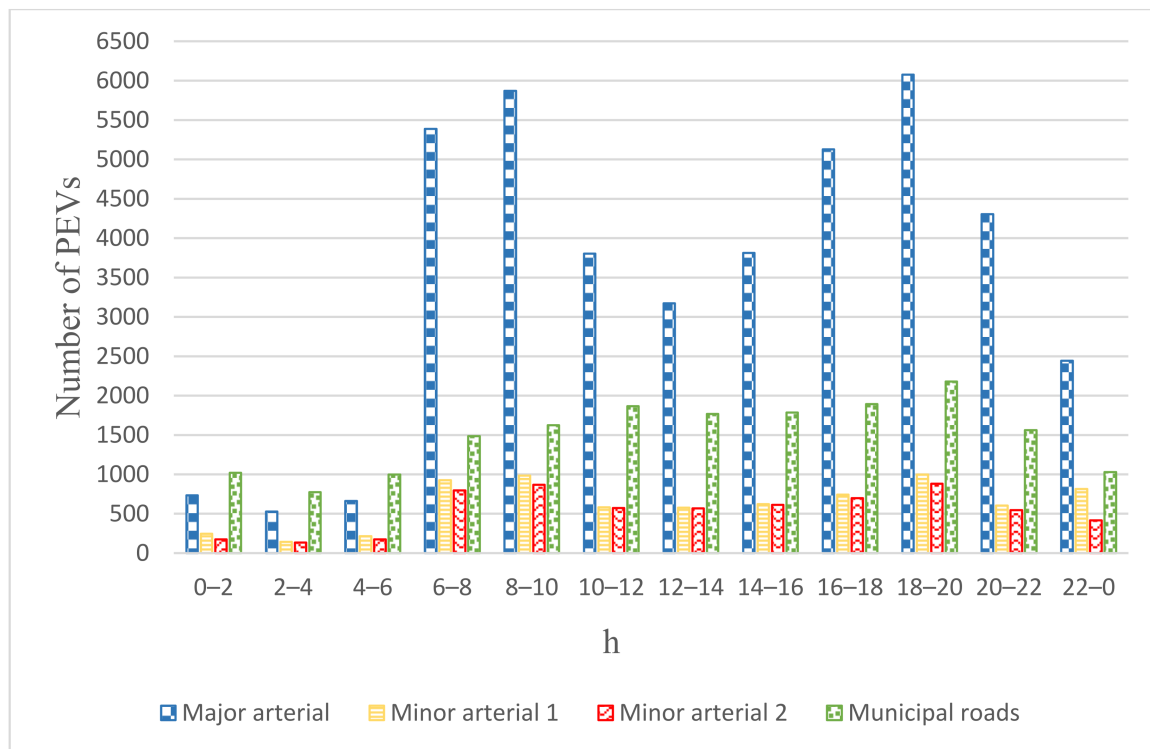
Figure 3. Illustration of traffic volumes in the original scenario.
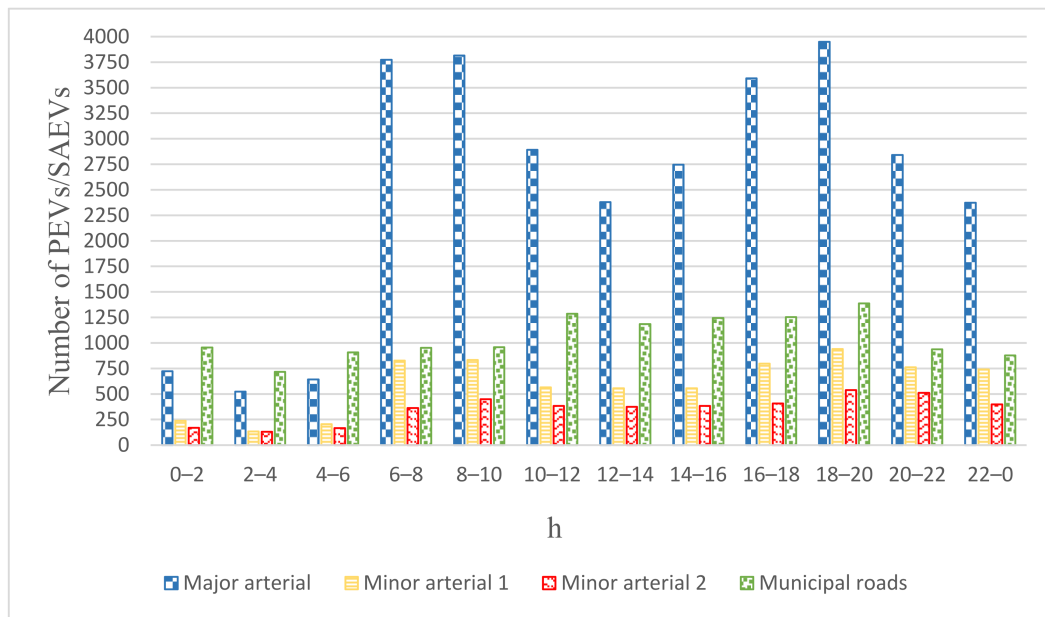
Figure 4 illustrates the average traversing times of the PEVs on all road sections before running the proposed algorithm. We assume parts of PEVs needed charging for their batteries during the trips. The charging time is also added into the total traversing time of a PEV that requires charging on its way to the destination. It can be seen that the serious traffic jams caused much longer time delays for the PEVs driving on the major arterial road during rush hours. We can image that most of the stuck EV users on the major arterial

road are the commuters on the way between their homes and workplaces. Most of the commuters also prefer taking the major arterial road that provides battery charging with the on-road charging to reduce their traversing times during rush hours. Notably, although the driving distance of minor arterial road 1 is slightly longer than that of minor arterial road 2, parts of PEV users switched their depleted batteries at the battery exchange service located at the intersection of minor arterial 2. The waiting and switching times taken by PEV users at the battery exchange service explains why the traversing time on minor arterial 1 is shorter than that on minor arterial 2 although the traffic volumes on minor arterial 1 are larger. In addition, the traversing time of a PEV driving on the municipal roads is significantly longer than that of the other three types owing to the lower driving speed limits and longer traffic light controls.
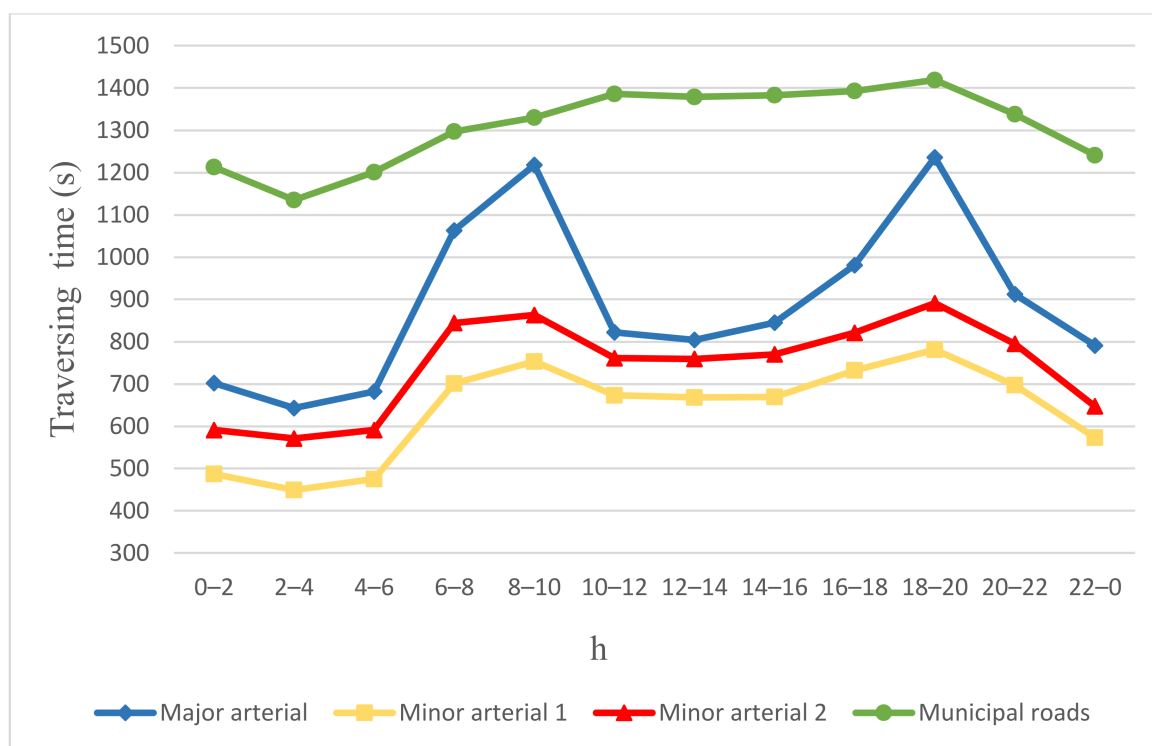
Figure 4. Illustration of traversing time of a PEV in the original scenario.

Figure 5 shows the traffic volumes of all road sections after rideshare companies support ridesharing service. Notably, we assume that each rideshare passenger took the rideshare serviced by the designated rideshare company via the APP installed on the cellphone. It can be seen that the traffic volumes of most road sections were reduced after parts of PEV users in the original scenario turned to take rideshare services. Nevertheless, the major arterial road was still the most crowded among all road sections during peak periods because most PEVs/SAEVs chose the fastest routes to their destinations, let alone the attractive time-saving on-road charging facility offered on the major arterial road. Notably, although a major portion of PEV users in the original scenario turned to take rideshare services, some of them cannot be served by their designated rideshare companies during rush hours due to the tight schedules of their SAEVs. Accordingly, the ones that cannot postpone their trip schedules still need to drive their own PEVs during peak periods and take the major arterial road as part of the routes to their destinations. In addition, the passengers that need the rideshare service are much fewer during off-peak periods and the number of the sharable routes are thus fewer than those during peak periods. Consequently, compared with Figure 3, no noticeable reduction of the traffic volumes during off-peak periods is observed in Figure 5.
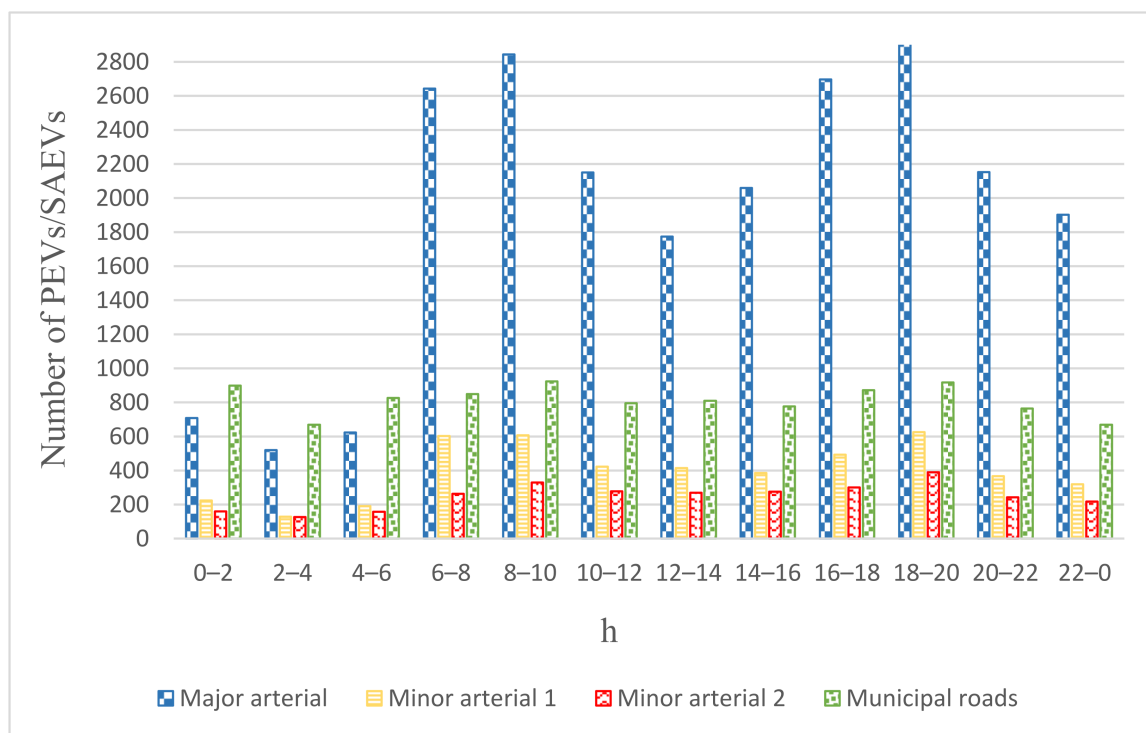
Figure 5. Traffic volumes of all road sections after rideshare companies support ridesharing service.

Figure 6 illustrates the traversing times of PEVs/SAEVs on all road sections after rideshare companies support ridesharing service. In comparison with Figure 4, the traversing times of PEVs/SAEVs at the major arterial road, minor arterial 1, minor arterial 2, and municipal roads after rideshare companies support ridesharing service decreased 12%, 15%, 14%, and 16% in average, respectively. Although the traversing times of PEVs/SAEVs were cut down due to the reduction in the vehicle numbers on all road sections, the traffic jam problem was still serious on the major arterial road during rush hours. The majority of the vehicles on the major arterial road were the PEVs owned by the commuters, who are either accustomed to taking the major arterial road as the major portion of the routes between their homes and workplaces, or unable to find any available rideshare services during rush hours because of the busy schedules of SAEV fleets.
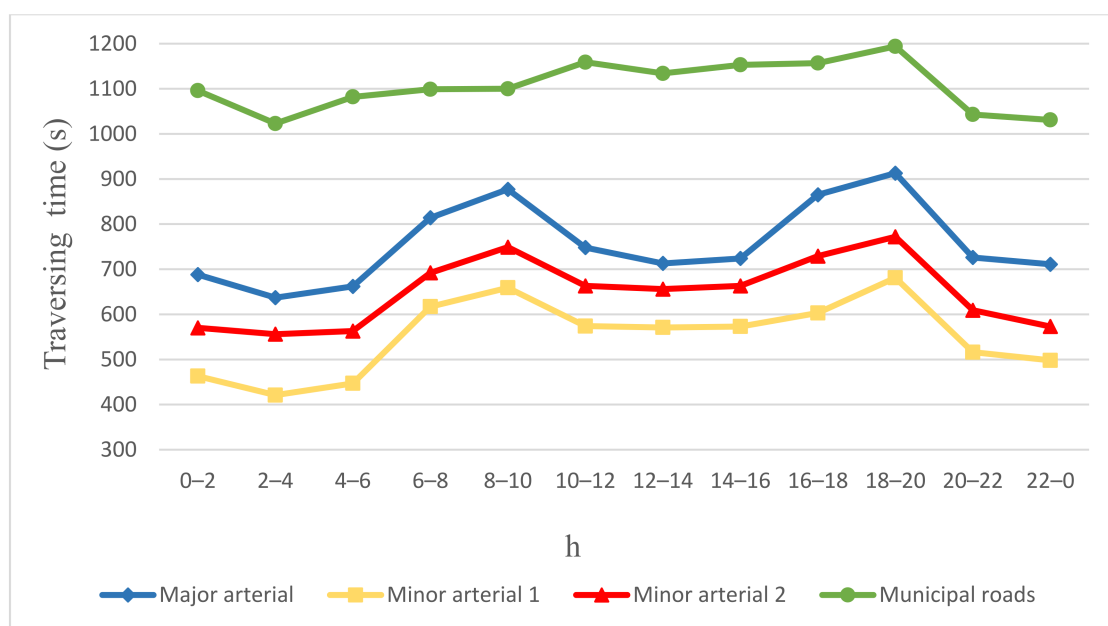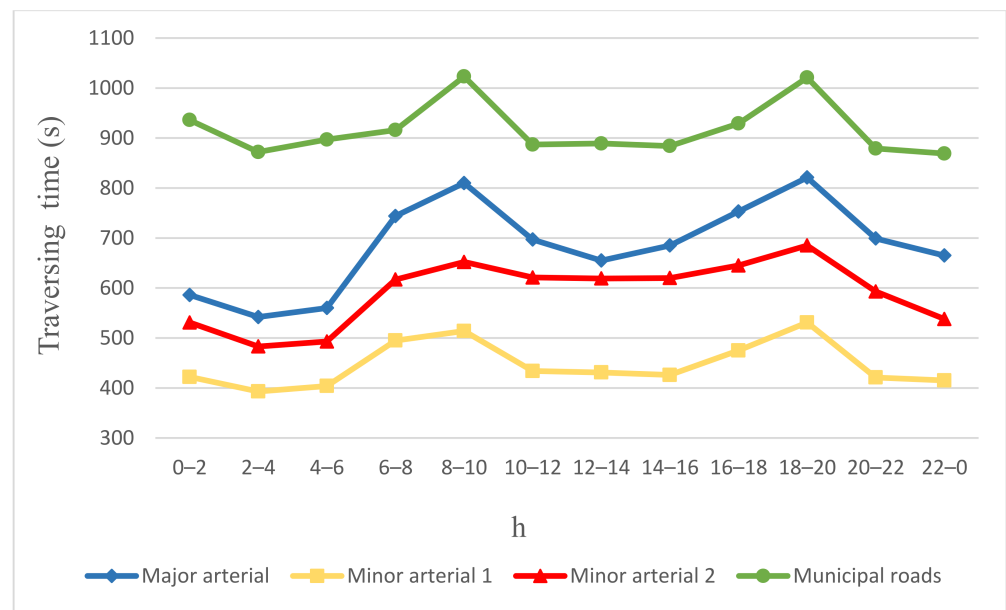

Figure 6. Traversing times of PEVs/SAEVs after rideshare companies support ridesharing service.

Next, we evaluate the effect of the proposed real time rideshare coordination mechanism. It was observed from Figure 5 that the rideshare requests from part of rideshare passengers were turned down during peak periods because the rideshare companies designated by the requesters were fully booked. After receiving the declined bookings from the rideshare companies, the proposed rideshare coordination mechanism attempts to match the declined bookings with all available rideshare routes posted by all rideshare companies. Accordingly, as shown in Figure 7, the traffic volumes of most road sections were further reduced after more PEV users in the original scenario were able to take rideshare services with the help of the proposed rideshare coordination mechanism. However, the congestion on the main arterial road was still severe because most of PEVs/SAEVs preferred taking the main arterial road during peak periods.
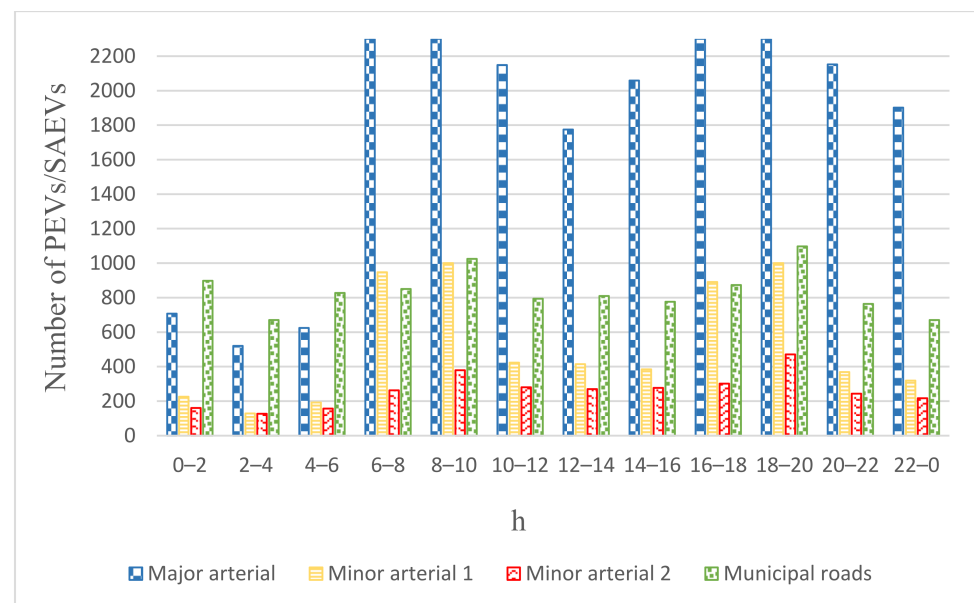

Figure 7. Traffic volumes of all road sections after applying real time rideshare coordination.

Figure 8 shows the traversing times of PEVs/SAEVs on all road sections after applying the proposed rideshare coordination mechanism. Compared with Figure 6, it can be observed that the traversing times of PEVs/SAEVs at the major arterial, minor arterial 1, minor arterial 2, and municipal roads after applying real time rideshare coordination decreased by 9%, 16%, 15%, and 17% in average, respectively. The average traversing times of PEV/SAEV passengers were further reduced because less congested traffic shortens the traversing times of PEV/SAEV passengers. However, the traffic jams over the major arterial road were not yet relieved because the major arterial road was chosen by all PEVs/SAEVs that can route via the major arterial road to the destinations. Accordingly, traffic volumes of PEVs/SAEVs that route via the major arterial road were still significantly larger than the two minor arterial roads, and surely elongated the traversing times of PEV/SAEV passengers.

Figure 8. Traversing times of PEVs/SAEVs after applying real time rideshare coordination.
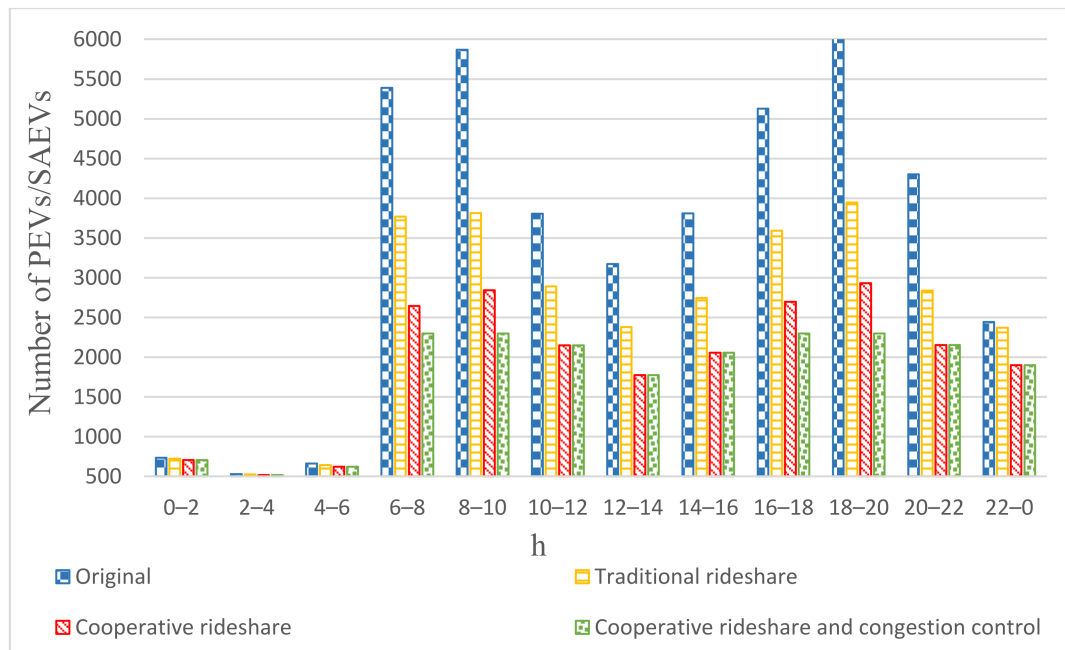
Figure 9 shows the traffic volumes of PEVs/SAEVs after activating the proposed real-time traffic volume surveillance mechanism. Compared with Figure 7, it can be observed that the traffic volumes during off-peak hours in both figures are alike. The traffic volume of the major arterial road after applying real time rideshare coordination during peak periods decreased, whereas the PEVs/SAEVs that were not permitted to take the main arterial road were diverted to the other three types of the road sections during peak periods. The percentages of the traffic volumes on the main arterial road diverted to minor arterial 1, minor arterial 2, and municipal roads during peak periods were 2%, 1%, and 3%, respectively.


Figure 9. Traffic volumes of all road sections after enforcing real-time traffic volume surveillance.

Figures 10–13 illustrate the differences of the traffic volumes on each type of road under the four above-mentioned scenarios. It can be seen from Figure 10 that the traffic volumes on the major arterial road during peak periods were flatten to the upper limit set by the

real-time traffic volume surveillance mechanism. Meanwhile, as shown in Figures 11–13, parts of traffic loads during peak periods were navigated into the two minor arterial roads and the surrounding municipal roads during the two commute peak hours. Nevertheless, traffic flows on the two minor arterial and the municipal roads were reduced owing to the effectiveness of rideshare coordination mechanism. In addition, the congestion pricing policy was also credited for the cut down of the traffic volume because some portion of PEV users were willing to take public transport as the alternative because of the shorter time and the lower expense.

Figure 10. Traffic volumes of PEV/SAEV passengers on the major arterial road.
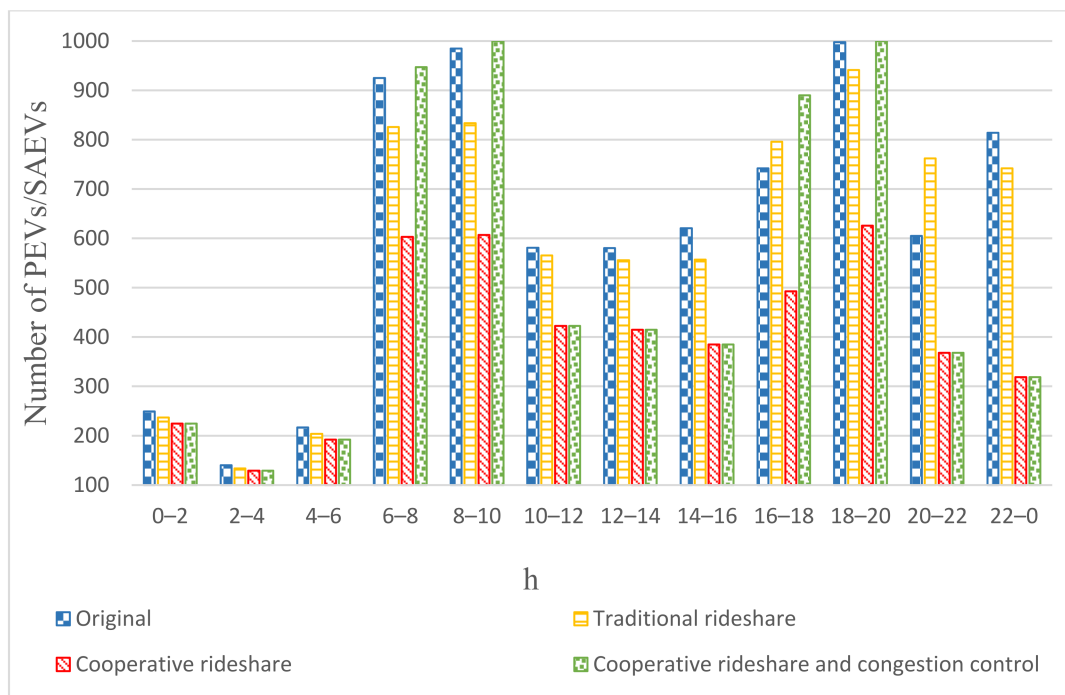
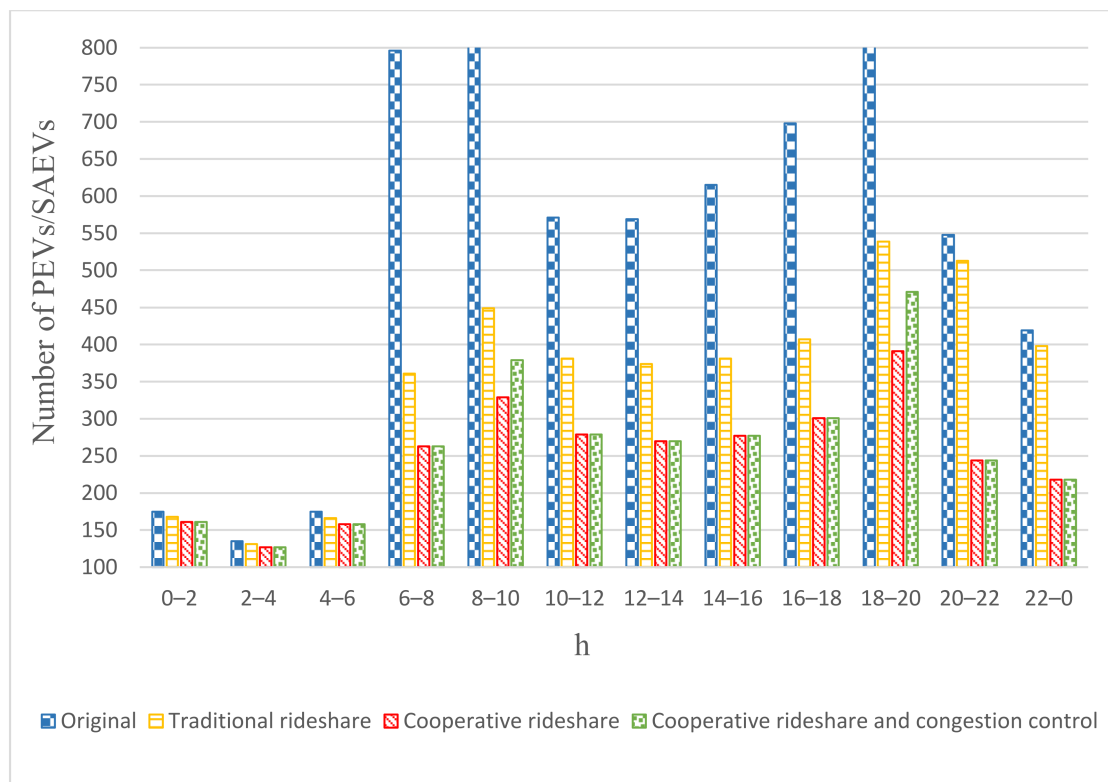**Figure 11.** Traffic volumes of PEV/SAEV passengers on minor arterial 1.

Figure 12. Traffic volumes of PEV/SAEV passengers on minor arterial 2.
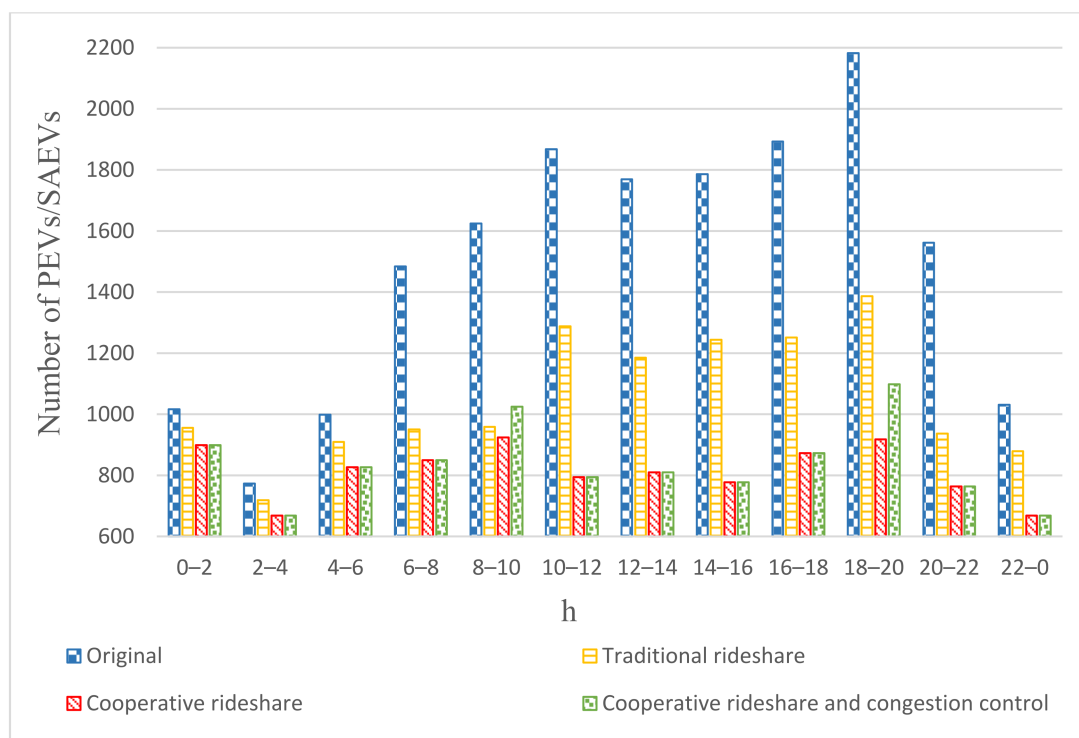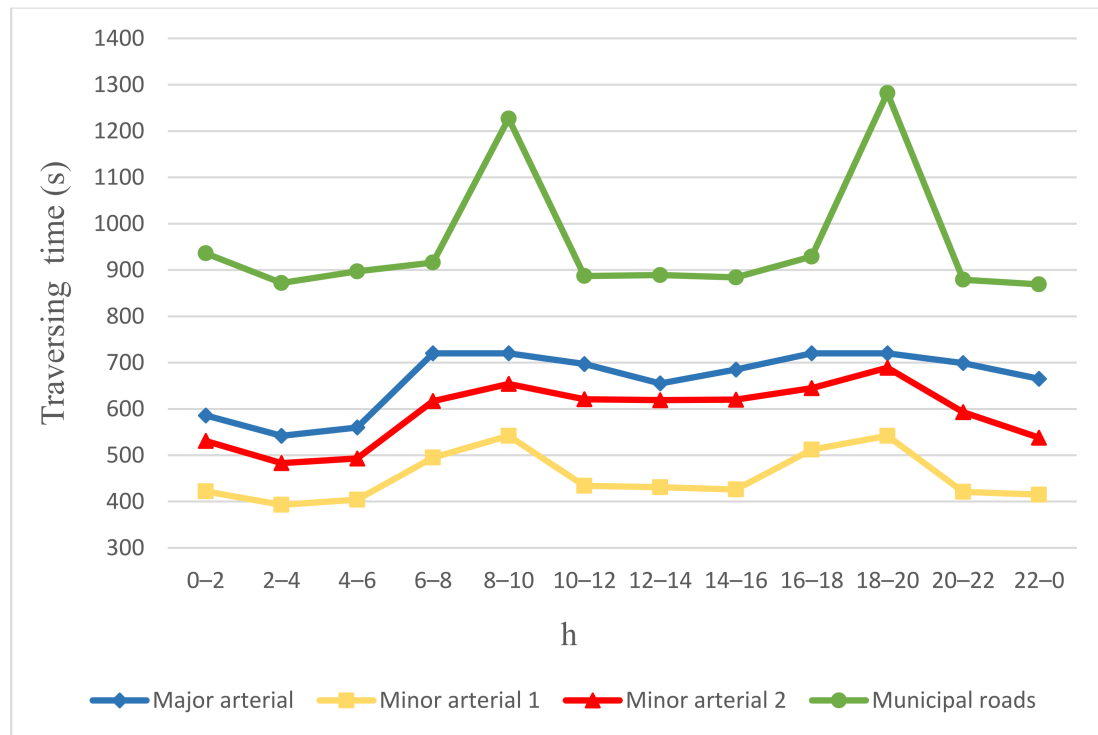

Figure 13. Traffic volumes of PEV/SAEV passengers on the municipal roads.

Figure 14 compares the traversing times of PEVs/SAEVs over four types of road sections after the real-time traffic volume surveillance mechanism was activated. The curve for the travelling times of PEVs/SAEVs observed on the major arterial road was much

flattened than that before traffic monitoring strategies was applied. Compared with Figure 8, it can be observed that the traversing times during off-peak hours in both figures were alike. The traversing times of PEVs/SAEVs at the major arterial after applying real time rideshare coordination during peak hours decreased by 8%. However, the traversing times of PEVs/SAEVs at minor arterial 1, minor arterial 2, and municipal roads increased by 3%, 2%, and 6%, respectively. The slight increase in the traversing times on the two minor arterial roads and the surrounding municipal roads were caused by the deviated PEVs/SAEVs owing to the declined route bookings of PEVs/SAEVs over the major arterial road.

Figure 14. Traversing times of PEVs/SAEVs after enforcing real-time traffic volume surveillance.

Figure 15 illustrates the traveling times of PEV/SAEV passengers for four different scenarios. In comparison to the original scenario, the average traveling times of PEVs/SAEV users for traditional rideshare, cooperative rideshare, and cooperative rideshare along with urban congestion control decreased by 14%, 26%, and 28% respectively. The traveling time for a PEV/SAEV user during peak periods is significantly longer that that during off-peak periods, even if the traditional rideshare services were offered by rideshare companies. Although part of the PEV users were inclined to take the rideshare alternative of the transportation during commuting time, the busy schedules of SAEV fleets operated by the rideshare companies during rush hours still forced some citizens to commute with their own PEVs. After the rideshare coordination mechanism was applied, it can be seen that the average traveling times for PEV/SAEV users were further cut down due to the effective matching of SAEV passengers with the suitable rideshare routes offered by some other rideshare company rather than the one that SAEV passengers designated.
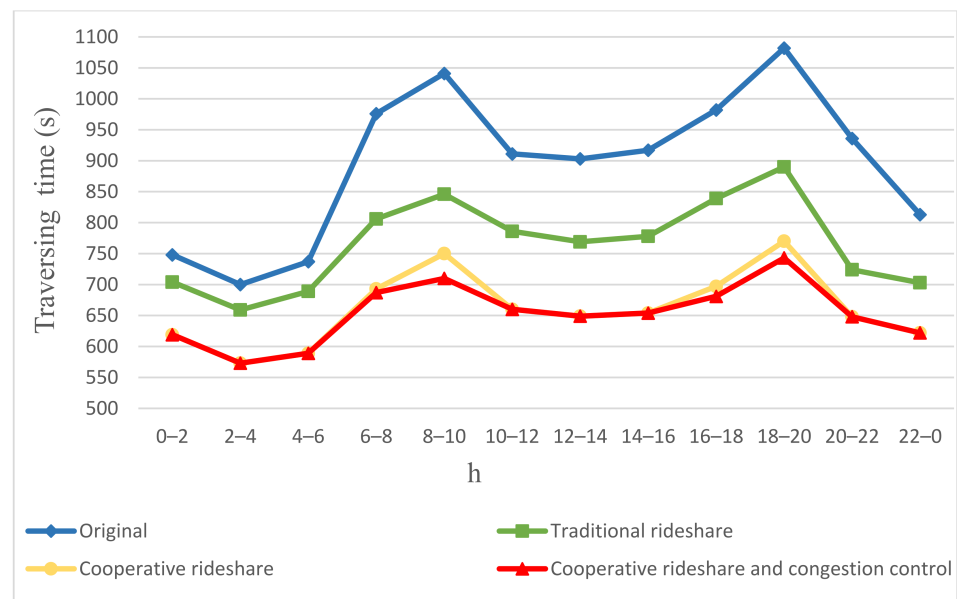
Figure 15. Traveling times of PEV/SAEV users for four different scenarios.

Figures 16–19 show the differences of the traversing times of PEV/SAEV passengers on each type of road under the four above-mentioned scenarios. It can be observed from Figure 16 that the serious traffic congestion was avoided on the major arterial road after applying the collaboration of the rideshare coordination and the real-time traffic volume surveillance. Accordingly, the average traversing times of PEV/SAEV passengers was the shortest among all the four scenarios. As shown in Figures 17–19, some PEV users were forced to take the minor arterial road(s) and/or the surrounding municipal roads during commuting hours; the significant reduction in the traversing time over the major arterial road compensated for the increased traversing times on other alternative road sections.
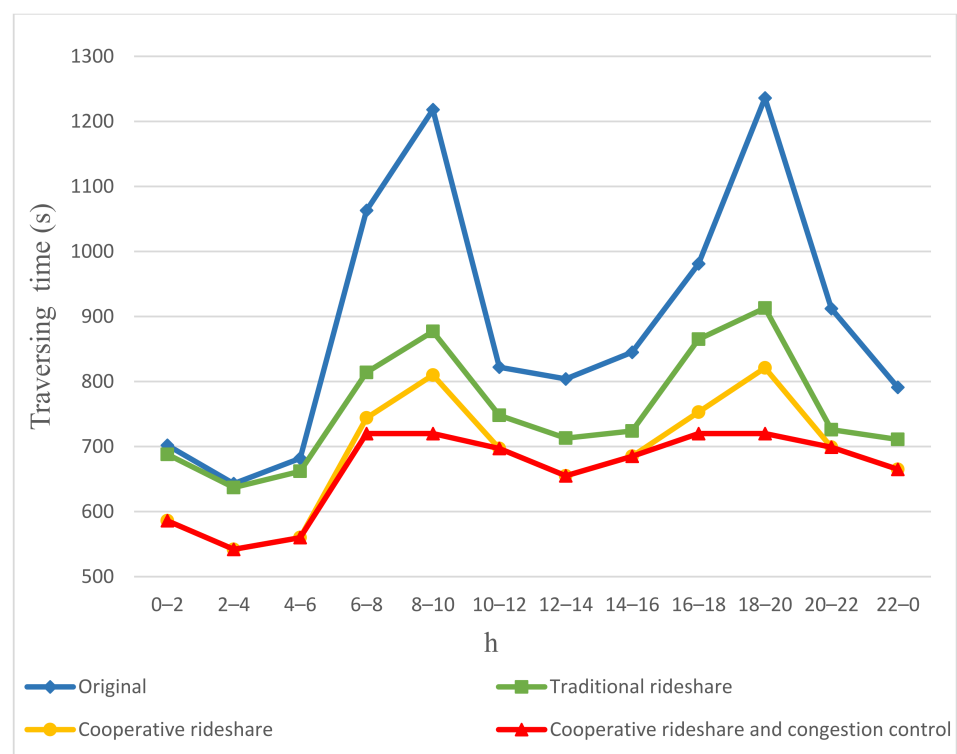
Figure 16. Traversing times of PEV/SAEV passengers on the major arterial road.
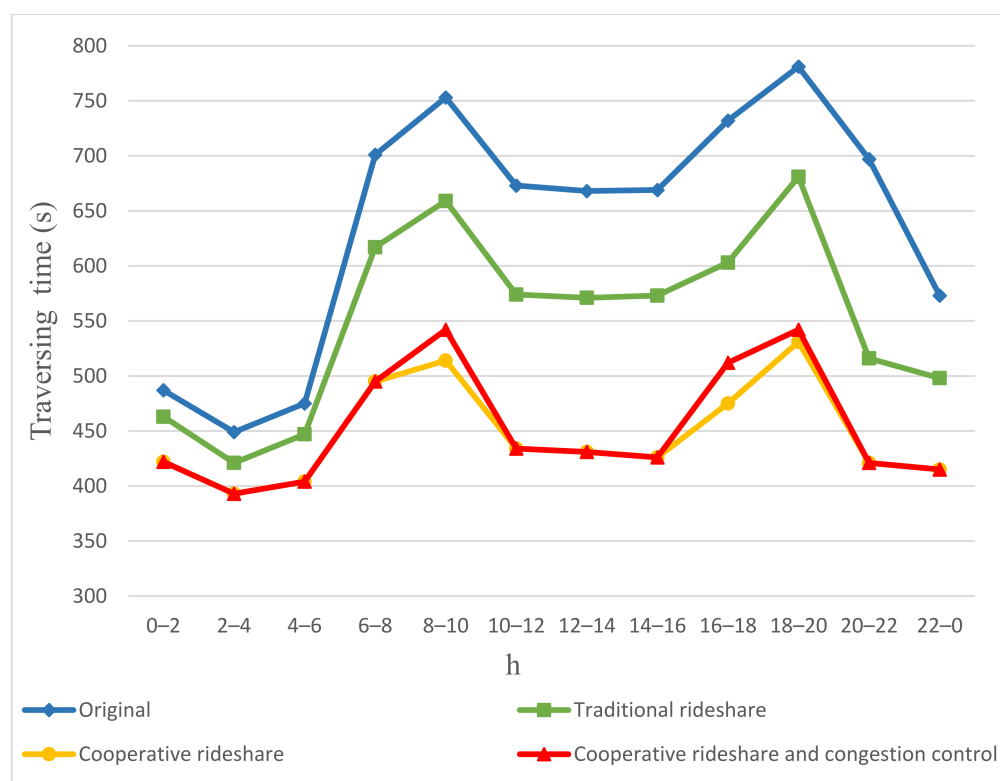
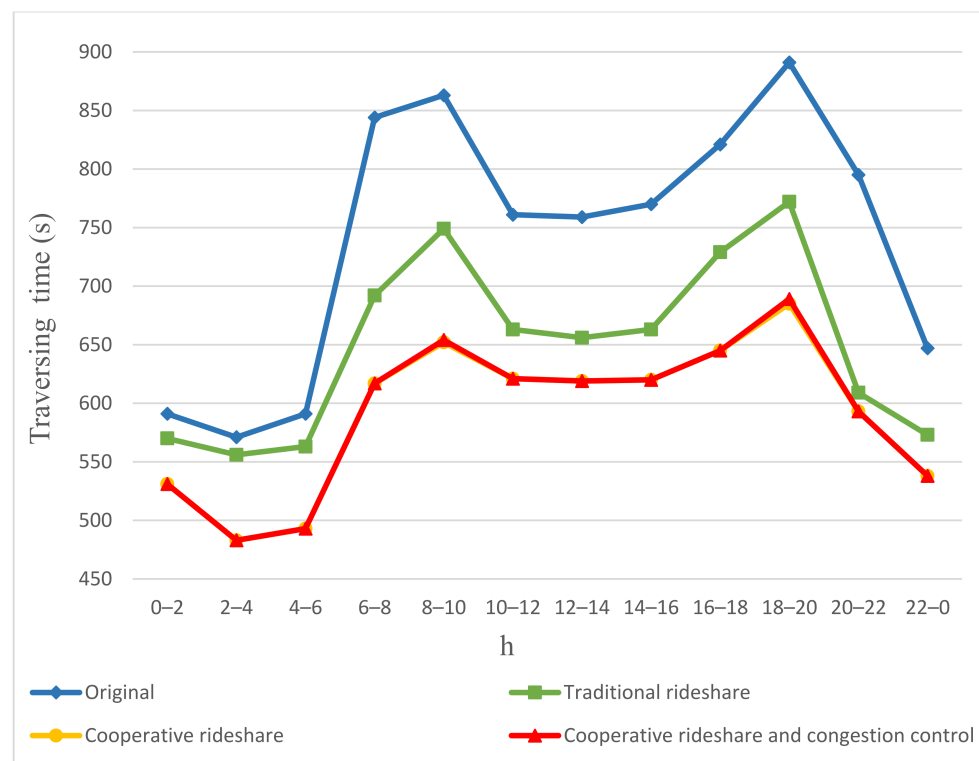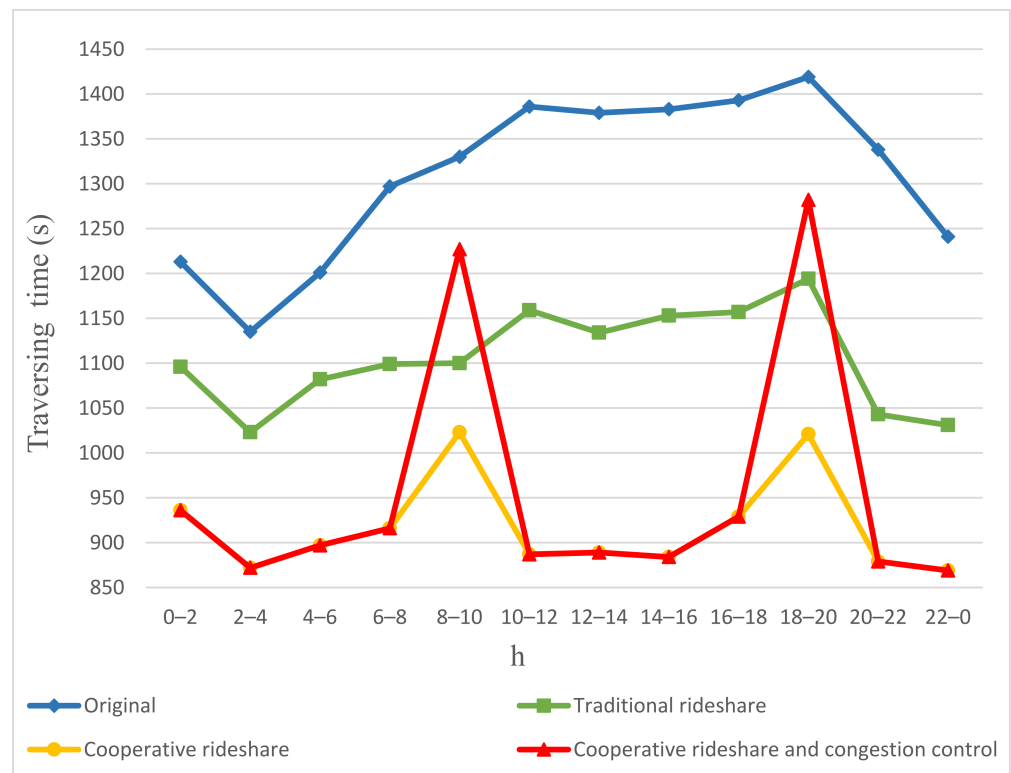**Figure 17.** Traversing times of PEV/SAEV passengers on minor arterial 1.

Figure 18. Traversing times of PEV/SAEV passengers on minor arterial 2.

Figure 19. Traversing times of PEV/SAEV passengers on the municipal roads.

5. Conclusions

In the literature, little research has proposed effective solutions that integrate the route of charging strategies for SAEV fleets with the urban traffic congestion problem. This work presents an integrated framework that tackles the route and charging of PEVs and SAEV fleets as well as the urban traffic congestion prevention issues. Real-time traffic volume surveillance is operated at the designated busy road sections, and flow redistribution is manipulated to reduce the traffic loads of busy roads. A PEV user first books a route ahead using the cellphone before her/his departure. Alternatively, a PEV user that is about to depart or is on the way to the destination can also use an on-road routing module installed at the OBU on the PEV to look for a preferred route in real time. The PEV user that is unable to find a satisfactory route to their destinations, along with the EV passenger that prefers taking the rideshare option, can use an APP to book a rideshare from the selected rideshare company, such as Uber or Lyft. In case the designated rideshare company cannot find any suitable rideshare that fits a passenger's request, a rideshare coordinator can assist in matching passengers' rideshares from other rideshare companies. Notably, effective heuristics were proposed to tackle the optimization problems of the above-mentioned framework in real time. The feasibility and effectiveness of the proposed algorithms was evaluated through four different scenarios in the simulation. After applying the proposed algorithms, it can be observed that the traffic volumes of the oversaturated main arterial road were diverted to less busy minor arterial and local municipal roads. The traveling times of EV passengers were decreased by 28% during peak time periods. The simulation results indicate that the proposed algorithms not only provide a joint solution for the problems of urban traffic congestion control and rideshare dispatch of SAEV fleets, but also fill the gap of the routing and charging strategies for mixed PEV and SAEV fleets in the literature.

Nomenclature

c_1^l	Origin of the route indexed by l
$c_{i'}^l$	ith intersection of the route indexed by l
$c_{h_l}^l$	Final destination of the route indexed by l
ω_1^l	Weight of the first parameter on the minimization objective in Equation (1)
ω_2^l	Weight of the second parameter on the minimization objective in Equation (1)
ω_3^l	Weight of the third parameter on the minimization objective in Equation (1)
ω_4^l	Weight of the fourth parameter on the minimization objective in Equation (1)
$sl_{c_i^l, c_{i+1}^l}$	Road length the road section between c_i^l and c_{i+1}^l
$rt_{c_i^l}$	Arrival time of the PEV at c_i
rt_{Org}	Departure time at the origin
rt_{Dst}^{max}	Deadline to reach the destination
K	Number of candidate routes kept by the PEV user
K^{max}	Preset maximal number of candidate route records saved by the PEV user
$cp_{c_i^l, c_{i+1}^l}\left(rt_{c_i^l}\right)$	Congestion pricing policy enforced on the road section between c_i^l and c_{i+1}^l at the time $rt_{c_i^l}$
$SD_{c_i^l, c_{i+1}^l}(t)$	Time of the PEV taking the road section between c_i^l and c_{i+1}^l at time t
$ID_{c_i^l, c_{i+1}^l}(t)$	Delay of the PEV while it reaches the intersection c_i at time t
SOC^{max}	Maximal PEV battery capacity
SOC^{min}	Minimal PEV battery capacity
$SoC_{c_i^l}$	PEV battery capacity when the PEV reaches c_i^l
$\phi_{c_i^l}$	Plug and charge station indexed by c_i^l that provides battery charging service for the PEV
$\Psi_{c_i^l}$	Battery exchange service indexed by c_i^l that provides battery charging service for the PEV
$\theta_{c_i^l, c_{i+1}^l}$	Electric road charging between c_i^l and c_{i+1}^l that provides battery charging service for the PEV
$RP_{c_i^l}(t)$	Real-time charging electricity price of the plug & charge or battery exchange service indexed by c_i^l at time t
$WP_{c_i^l, c_{i+1}^l}(t)$	Charging price for electric road on the section connecting c_i^l and c_{i+1}^l at time t
$pcp_{c_i^l}$	Battery charging power/sec for the plug & charge station indexed by c_i^l
$wcp_{c_i^l, c_{i+1}^l}$	Battery charging power/sec for electric road on the section connecting c_i^l and c_{i+1}^l
$ct_{c_i^l}$	Actual battery charging time of the PEV at the plug & charge station c_i^l
$ct_{c_i^l}^{max}$	Maximal battery charging time of the PEV at the plug & charge station c_i^l
$BSD_{c_i^l}(t)$	Time for an PEV takes the battery exchange service provided by c_i^l at time t
ap	PEV's battery power consumption per kilometer
η	Charging efficiency of an PEV's battery
$\xi_{c_i^l, c_{i+1}^l}\left(rt_{c_i^l}\right)$	Binary flag that controls the traffic of the road section connecting c_i^l and c_{i+1}^l at the time $rt_{c_i^l}$
$cm_{c_i^l, c_{i+1}^l}$	Binary flag that indicates if the road section between c_i^l and c_{i+1}^l is not congested
π	Binary flag that indicates if the booking is made in advance or the EV is about to head for the destination without making reservation first
$\rho_{c_i^l, c_{i+1}^l}^{rb}\left(\tau_{c_i^l, c_{i+1}^l}\right)$	Updated traffic density for route bookings of PEVs at the road section connecting c_i^l and c_{i+1}^l during the future interval starting at time $\tau_{c_i^l, c_{i+1}^l}$

$\rho^{rr}_{c^l_i,c^l_{i+1}}\left(\tau_{c^l_i,c^l_{i+1}}\right)$	Updated traffic density for on-road routings of PEVs at the road section connecting c^l_i and c^l_{i+1} during the future interval starting at time $\tau_{c^l_i,c^l_{i+1}}$
$\rho^{rb,max}_{c^l_i,c^l_{i+1}}\left(\tau_{c^l_i,c^l_{i+1}}\right)$	Maximal traffic density allowed for route bookings of PEVs at the road section connecting c^l_i and c^l_{i+1} during the future interval starting at time $\tau_{c^l_i,c^l_{i+1}}$
$\rho^{rr,max}_{c^l_i,c^l_{i+1}}\left(\tau_{c^l_i,c^l_{i+1}}\right)$	Maximal traffic density allowed for on-road routings of PEVs at the road section c^l_i and c^l_{i+1} during the future interval starting at time $\tau_{c^l_i,c^l_{i+1}}$
ci^l	Binary flag that indicates whether the lth route is not congested.
c^l_0	Index of the intersection just passed
c^l_1	Index of the closest intersection ahead on the route
$c^l_{v(l)}$	Index of the destination
Cur	Current location of the PEV
rt_{Cur}	Current time
$rt'_{c^l_i}$	Updated time that the PEV reaches the intersection c^l_i
sl_{Cur,c^l_i}	Distance between the current location and the closest intersection ahead
$df_{c^l_i,c^l_{i+1}}$	Binary flag that indicates whether the updated arrival time and the original time estimated during route booking is larger than a preset threshold $\delta_{c^l_i,c^l_{i+1}}$
$\delta_{c^l_i,c^l_{i+1}}$	Preset threshold time of the road section between c^l_i and c^l_{i+1}
σ	Index of the candidate route
c^σ_1	Index of the next intersection ahead
$c^\sigma_{v(\sigma)}$	Index of the next destination
$rt'_{c^\sigma_i}$	Updated time that the PEV reaches the intersection c^σ_i
$\rho^{rr}_{c^\sigma_i,c^\sigma_{i+1}}\left(\tau_{c^\sigma_i,c^\sigma_{i+1}}\right)$	Updated traffic density of the real-time traffic of PEVs on the road section that connects c^σ_i and c^σ_{i+1}
$\rho^{rr,max}_{c^\sigma_i,c^\sigma_{i+1}}\left(\tau_{c^\sigma_i,c^\sigma_{i+1}}\right)$	Maximal traffic density of the real-time traffic of PEVs allowed on the road section during the future interval starting at time $\tau_{c^\sigma_i,c^\sigma_{i+1}}$
ra^σ	Binary flag that indicates whether the alternative route is accessible
ev^{at}	Estimated arrival time of the PEV ev that requests for route cancellation during the current interval
ev^{id}	Identification number of the PEV ev that requests for route cancellation during the current interval
$BQ^{pre}_{l,m}$	Pointer to the previous record of the booked record for ev in the route-booking queue of the PEVs on the road section between l and m
at	Attribute of the arrival time of the PEV in the route-booking record
id	Attribute of the identification number of the PEV in the route-booking record
$next$	Attribute of pointer to the next record of the linked queue
st	Attribute of the route-booking queue that stands for the starting time of the fixed interval that the EV arrives at the road section
$\rho^{rb}_{l,m}(\tau_{l,m})$	Updated traffic density of the route-booking PEVs at the road section connecting l and m within a certain future interval starting at the time $\tau_{l,m}$
$delete(\cdot)$	Deletion function that removes the record from the linked queue.
$\mathcal{R}^\alpha_i$	ith route of a SAEV indexed by α
Φ	Total number of EVs operated by the designated rideshare company
P^Φ	Counts of α's rideshare routes
$r^\alpha_{i,1}$	Origin of the ith route assigned to fleet member α

$r^{\alpha}_{i,cp^{\alpha}_i}$	Last stop of the *i*th route assigned to fleet member α
$r^{\alpha}_{i,fp^{\alpha}_i}$	First pickup point on the *i*th route
$r^{\alpha}_{i,ld^{\alpha}_i}$	Last drop-off point on the *i*th route
$r^{\alpha}_{i,1}$	Charging point that can offer charging facilities for α when its battery capacity is estimated to fall below the minimal SOC during the next rideshare route
r_{i,cp^{α}_i}	Charging point that can offer charging facilities for α when its battery capacity is estimated to fall below the minimal SOC during the next rideshare route
$r^{\alpha}_{i+1,1}$	Starting node of the $(i+1)$th rideshare route
$\varpi^{\alpha}_{i,1}$	Weight of the rideshare passenger's first optimization objective in Equation (34)
$\varpi^{\alpha}_{i,2}$	Weight of the rideshare passenger's second optimization objective in Equation (34)
(x_s, y_s)	Rideshare passenger's departure location
(x_e, y_e)	Rideshare passenger's destination location
$r^{\alpha}_{i,pp^{\alpha}_i}$	Pickup point of the rideshare passenger
$r^{\alpha}_{i,dp^{\alpha}_i}$	Drop-off point of the rideshare passenger
$\left(x_{r^{\alpha}_{i,pp^{\alpha}_i}}, y_{r^{\alpha}_{i,pp^{\alpha}_i}} \right)$	Pickup point location of the rideshare passenger
$\left(x_{r^{\alpha}_{i,dp}}, y_{r^{\alpha}_{i,dp}} \right)$	Drop-off point location of the rideshare passenger
$rt_{r^{\alpha}_{i,pp^{\alpha}_i}}$	Arrival time for α to arrive at $r^{\alpha}_{i,pp^{\alpha}_i}$
$pt_{r^{\alpha}_{i,pp^{\alpha}_i}}$	Arrival time for the rideshare passenger to arrive at $r^{\alpha}_{i,pp^{\alpha}_i}$
δ^d	Maximal distance for the passenger to reach the pickup/drop-off point
δ^t	Maximal time that the passenger can wait at the pickup point
$r^{\alpha}_{i,cp^{\alpha,new}_i}$	Charging point at the end of the extended *i*th rideshare route
$pn^{cur}_{r^{\alpha}_{i,pp^{\alpha}_i}}$	Number of the riders on SAEV α before it reaches $r^{\alpha}_{i,pp^{\alpha}_i}$
$pn^{new}_{r^{\alpha}_{i,pp^{\alpha}_i}}$	Number of passengers α picks up at $r^{\alpha}_{i,pp^{\alpha}_i}$
$pn^{\alpha,max}$	α's maximal seating capacity
$\varpi^{\alpha}_{i,1}$	Weight of the first optimization objective set by the rideshare company in Equation (39)
$\varpi^{\alpha}_{i,2}$	Weight of the second optimization objective set by the rideshare company in Equation (39)
$\varpi^{\alpha}_{i,3}$	Weight of the third optimization objective set by the rideshare company in Equation (39)
$\mathcal{R}^{\alpha}_i$	*i*th rideshare route of SAEV α after accepting the new assignment of serving the rideshare requester(s)
$\mathcal{R}^{\alpha}_{i+1}$	$(i + 1)$th rideshare route of SAEV α after accepting the new assignment of serving the rideshare requester(s)
$r^{\alpha}_{i,fp^{\alpha}_i}$	The first pickup point of α's *i*th rideshare route before serving the new rideshare requester
$r^{\alpha}_{i,ld^{\alpha}_i}$	The last drop-off point of α's *i*th rideshare route before serving the new rideshare requester
$r^{\alpha}_{i,pp^{\alpha}_i}$	Pickup point of the new rideshare requester
$r^{\alpha}_{i,dp^{\alpha}_i}$	Drop-off point of the new rideshare requester
$r^{\alpha}_{i,cp^{\alpha,new}_i}$	Charging point at the end of the extended *i*th rideshare route
$r^{\alpha}_{i+1,1^{new}}$	New starting node on α's updated $(i+1)$th route

$r_{i+1,2^{new}}^{\alpha}$	The next intersection after new starting node on α's updated $(i+1)$th route
$SD_{r_{i,j}^{\alpha},r_{i,j+1}^{\alpha}}(t)$	Time SAEV α passes through the road section that between $r_{i,j}^{\alpha}$ and $r_{i,j+1}^{\alpha}$ at time t
$ID_{r_{i,j}^{\alpha},r_{i,j+1}^{\alpha}}(t)$	Delay time of α at the intersection $r_{i,j}^{\alpha}$ at time t
$\kappa_{r_{i,j}^{\alpha}}$	Binary flag that indicates if $r_{i,j}^{\alpha}$ is the pickup/drop off point
$PD_{r_{i,j}^{\alpha},r_{i,j+1}^{\alpha}}\left(pn_{r_{i,j}^{\alpha}}^{new}\right)$	Estimated delay for α to pick up/drop off $pn_{r_{i,j}^{\alpha}}^{new}$ rideshare passenger at $r_{i,j}^{\alpha}$
$pn_{r_{i,pp_i^{\alpha}}^{\alpha}}^{cur}$	Number of the riders that α carries when it reaches $r_{i,pp_i^{\alpha}}^{\alpha}$
$pn_{r_{i,pp_i^{\alpha}}^{\alpha}}^{new}$	Number of rideshare requesters picked up at $r_{i,pp_i^{\alpha}}^{\alpha}$
$pn^{\alpha,max}$	α's maximal seating capacity
$RP_{r_{i,1}^{\alpha}}\left(rt_{r_{i,1}^{\alpha}}\right)$	Real-time charging electricity price of the plug & charge or battery exchange service indexed by $r_{i,1}^{\alpha}$ at time $rt_{r_{i,1}^{\alpha}}$
$WP_{r_{i,j}^{\alpha},r_{i,j+1}^{\alpha}}\left(rt_{r_{i,j}^{\alpha}}\right)$	Real-time charging electricity price of the electric road charging on the road section connecting $r_{i,j}^{\alpha}$ and $r_{i,j+1}^{\alpha}$ at time $rt_{r_{i,j}^{\alpha}}$
$pcp_{r_{i,1}^{\alpha}}$	Charging power/second for the plug & charge station indexed by $r_{i,1}^{\alpha}$
$wcp_{r_{i,j}^{\alpha},r_{i,j+1}^{\alpha}}$	Charging power/second for the electric road charging offered by the road section connecting $r_{i,j}^{\alpha}$ and $r_{i,j+1}^{\alpha}$
$ct_{r_{i,1}^{\alpha}}^{max}$	Maximal charging time of the SAEV at the plug & charge station $r_{i,1}^{\alpha}$
$ct_{r_{i,1}^{\alpha}}$	Actual charging time of the SAEV at the plug & charge station $r_{i,1}^{\alpha}$
$sl_{r_{i,j}^{\alpha},r_{i,j+1}^{\alpha}}$	Road length between $r_{i,j}^{\alpha}$ and $r_{i,j+1}^{\alpha}$
$rt_{r_{i,pp_i^{\alpha}}^{\alpha}}$	Arrival time for SAEV α to arrive at $r_{i,pp_i^{\alpha}}^{\alpha}$
$pt_{r_{i,pp_i^{\alpha}}^{\alpha}}$	Arrival time for rideshare passenger to arrive at $r_{i,pp_i^{\alpha}}^{\alpha}$
$dt_{r_{i+1,1^{new}}^{\alpha}}$	α's departure time of the updated $(i+1)$th route
$SOC^{\alpha,max}$	Maximal battery capacity of SAEV α
$SOC^{\alpha,min}$	Minimal battery capacity of SAEV α
$SOC_{r_{i,1}^{\alpha}}^{\alpha}$	α's battery capacity when it reaches $r_{i,1}^{\alpha}$
$\phi_{r_{i,1}^{\alpha}}$	Binary flag that indicates if the plug & charge station located at $r_{i,1}^{\alpha}$ is chosen for recharging
$\Psi_{r_{i,1}^{\alpha}}$	Binary flag that indicates if the battery exchange service located at $r_{i,1}^{\alpha}$ is chosen for recharging
$\theta_{r_{i,j},r_{i,j+1}}$	Binary flag that indicates if the electric road charging provided on the road section connecting $r_{i,j}^{\alpha}$ and $r_{i,j+1}^{\alpha}$ is used to charge for α's battery
ap^{α}	Power consumption of α's battery per kilometer
η^{α}	Charging efficiency of α's battery
$\rho_{r_{i,j}^{\alpha},r_{i,j+1}^{\alpha}}^{rf}\left(\tau_{r_{i,j}^{\alpha},r_{i,j+1}^{\alpha}}\right)$	Current traffic density for the traffic flow of SAEVs during the future interval starting at time $\tau_{r_{i,j}^{\alpha},r_{i,j+1}^{\alpha}}$
$\rho_{r_{i,j}^{\alpha},r_{i,j+1}^{\alpha}}^{rf}\left(\tau_{r_{i,j}^{\alpha},r_{i,j+1}^{\alpha}}\right)$	Maximal traffic density for the traffic flow of SAEVs during the future interval starting at time $\tau_{r_{i,j}^{\alpha},r_{i,j+1}^{\alpha}}$,
$\mathcal{R}_i^{k,\alpha}$	ith route of SAEV α operated by the rideshare company indexed by k
Θ	Number of rideshare companies
Φ^k	Total number of EVs operated by the rideshare company k
$\mathrm{P}^{k,\alpha}$	Number of α's rideshare routes assigned by rideshare company k
$r_{i,1}^{k,\alpha}$	Origin of the ith route assigned to α
$r_{i,cp_i^{k,\alpha}}^{k,\alpha}$	Last stop of the ith route assigned to α

$r^{k,\alpha}_{i,fp^{k,\alpha}_i}$	The first pickup point on the ith route of α
$r^{k,\alpha}_{i,ld^{k,\alpha}_i}$	The last drop-off point on the ith route of α
$\varpi^{k,\alpha}_{i,1}$	Weight of the rideshare passenger's first optimization objective in Equation (56)
$\varpi^{k,\alpha}_{i,2}$	Weight of the rideshare passenger's second optimization objective in Equation (56)
$r^{k,\alpha}_{i,pp^{k,\alpha}_i}$	Pickup point designated in Equation (56)
$r^{k,\alpha}_{i,dp^{k,\alpha}_i}$	Drop-off point designated in Equation (56)
$\left(x_{r^{k,\alpha}_{i,pp^{k,\alpha}_i}}, y_{r^{k,\alpha}_{i,pp^{k,\alpha}_i}}\right)$	Location of the pickup point designated in Equation (56)
$\left(x_{r^{k,\alpha}_{i,dp^{k,\alpha}_i}}, y_{r^{k,\alpha}_{i,dp^{k,\alpha}_i}}\right)$	Location of the drop-off point designated in Equation (56)
$rt_{r^{k,\alpha}_{i,pp^{k,\alpha}_i}}$	Arrival time for SAEV α to arrive at $r^{k,\alpha}_{i,pp^{k,\alpha}_i}$
$pt_{r^{k,\alpha}_{i,pp^{k,\alpha}_i}}$	Arrival time for the rideshare passenger to arrive at $r^{k,\alpha}_{i,pp^{k,\alpha}_i}$
$pn^{cur}_{r^{k,\alpha}_{i,pp^{k,\alpha}_i}}$	Number of the passengers that SAEV α carries after it reaches $r^{k,\alpha}_{i,pp^{k,\alpha}_i}$
$pn^{new}_{r^{k,\alpha}_{i,pp^{k,\alpha}_i}}$	Number of rideshare requester(s) picked up at $r^{k,\alpha}_{i,pp^{k,\alpha}_i}$
$pn^{k,\alpha,max}$	Maximal seating capacity of α
$rt_{r^{k,\alpha}_{i,ld^{k,\alpha}_i}}$	The time that SAEV α leaves the last drop-off point of its ith route
$rt_{r^{k,\alpha}_{i+1,fp^{k,\alpha}_{i+1}}}$	The time that SAEV α arrives at the first pickup point of its $(i+1)$th route

References

1. Ritchie, H. Urbanization. 2018. Available online: https://ourworldindata.org/urbanization (accessed on 12 January 2022).
2. Vosooghi, R.; Puchinger, J.; Bischoff, J.; Jankovic, M.; Vouillon, A. Shared autonomous electric vehicle service performance: Assessing the impact of charging infrastructure. *Transp. Res. Part D Transp. Environ.* **2020**, *81*, 102283. [CrossRef]
3. Narayanan, S.; Chaniotakis, E.; Antoniou, C. Shared autonomous vehicle services: A comprehensive review. *Transp. Res. Part C Emerg. Technol.* **2020**, *111*, 255–293. [CrossRef]
4. Joo, H.; Ahmed, S.H.; Lim, Y. Traffic signal control for smart cities using reinforcement learning. *Comput. Commun.* **2020**, *154*, 324–330. [CrossRef]
5. Kumar, N.; Rahman, S.S.; Dhakad, N. Fuzzy inference enabled deep reinforcement learning-based traffic light control for intelligent transportation system. *IEEE Trans. Intell. Transp. Syst.* **2021**, *22*, 4919–4928. [CrossRef]
6. Rasheed, F.; Yau KL, A.; Low, Y.C. Deep reinforcement learning for traffic signal control under disturbances: A case study on Sunway city, Malaysia. *Future Gener. Comput. Syst.* **2020**, *109*, 431–445. [CrossRef]
7. Wang, H.; Zhu, M.; Hong, W.; Wang, C.; Tao, G.; Wang, Y. Optimizing Signal Timing Control for Large Urban Traffic Networks Using an Adaptive Linear Quadratic Regulator Control Strategy. *IEEE Trans. Intell. Transp. Syst.* **2022**, *23*, 333–343. [CrossRef]
8. Du, Y.; ShangGuan, W.; Chai, L. A coupled vehicle-signal control method at signalized intersections in mixed traffic environment. *IEEE Trans. Veh. Technol.* **2021**, *70*, 2089–2100. [CrossRef]
9. Hou, Z.; Lei, T. Constrained Model Free Adaptive Predictive Perimeter Control and Route Guidance for Multi-Region Urban Traffic Systems. *IEEE Trans. Intell. Transp. Syst.* **2022**, *23*, 912–924. [CrossRef]
10. Li, D.; De Schutter, B. Distributed model-free adaptive predictive control for urban traffic networks. *IEEE Trans. Control. Syst. Technol.* **2022**, *30*, 180–192. [CrossRef]
11. Zhang, Y.; Zhou, Y.; Lu, H.; Fujita, H. Spark cloud-based parallel computing for traffic network flow predictive control using non-analytical predictive model. *IEEE Trans. Intell. Transp. Syst.* **2022**, *23*, 7708–7720. [CrossRef]
12. Hosseinzadeh, M.; Sinopoli, B.; Kolmanovsky, I.; Baruah, S. MPC-Based Emergency Vehicle-Centered Multi-Intersection Traffic Control. In *IEEE Transactions on Control Systems Technology*; IEEE: Piscataway, NJ, USA, 2022.
13. Zuo, Z.; Yang, X.; Li, Z.; Wang, Y.; Han, Q.; Wang, L.; Luo, X. MPC-based cooperative control strategy of path planning and trajectory tracking for intelligent vehicles. *IEEE Trans. Intell. Veh.* **2021**, *6*, 513–522. [CrossRef]
14. Wang, Z.; Wang, S. Real-time Dynamic Route Optimization Based on Predictive Control Principle. *IEEE Access* **2022**, *10*, 55062–55072. [CrossRef]

15. Chen, Y.; Zheng, N.; Vu, H.L. A novel urban congestion pricing scheme considering travel cost perception and level of service. *Transp. Res. Part C Emerg. Technol.* **2021**, *125*, 103042. [CrossRef]

16. Baghestani, A.; Tayarani, M.; Allahviranloo, M.; Gao, H.O. Evaluating the Traffic and Emissions Impacts of Congestion Pricing in New York City. *Sustainability* **2020**, *12*, 3655. [CrossRef]

17. Genser, A.; Kouvelas, A. Dynamic optimal congestion pricing in multi-region urban networks by application of a Multi-Layer-Neural network. *Transp. Res. Part C Emerg. Technol.* **2022**, *134*, 103485. [CrossRef]

18. Abulibdeh, A. Planning for congestion pricing policies in the middle east: Public acceptability and revenue distribution. *Transp. Lett.* **2022**, *14*, 282–297. [CrossRef]

19. Baghestani, A.; Tayarani, M.; Allahviranloo, M.; Nadafianshahamabadi, R.; Kucheva, Y.; Mamdoohi, A.R.; Gao, H.O. New York City cordon pricing and its' impacts on disparity, transit accessibility, air quality, and health. *Case Stud. Transp. Policy* **2022**, *10*, 485–499. [CrossRef]

20. Guo, Y.; Li, Y.; Anastasopoulos, P.C.; Peeta, S.; Lu, J. China's millennial car travelers' mode shift responses under congestion pricing and reward policies: A case study in Beijing. *Travel Behav. Soc.* **2021**, *23*, 86–99. [CrossRef]

21. Abbasi, M.; Piccioni, C.; Sarreshtehdari, A.; Lee, Y.J. Modeling travel mode choice under the effect of congestion pricing: The case study of Tehran. *Adv. Transp. Stud.* **2022**, *56*, 89–106.

22. Golbabaei, F.; Yigitcanlar, T.; Bunker, J. The role of shared autonomous vehicle systems in delivering smart urban mobility: A systematic review of the literature. *Int. J. Sustain. Transp.* **2021**, *15*, 731–748. [CrossRef]

23. Huo, X.; Wu, X.; Fan, Y.; Ding, C. A Mixed-Integer Program (MIP) for One-Way Multiple-Type Shared Electric Vehicles Allocation with Uncertain Demand. *IEEE Trans. Intell. Transp. Syst.* **2022**, *23*, 8972–8984. [CrossRef]

24. Haliem, M.; Mani, G.; Aggarwal, V.; Bhargava, B. A distributed model-free ride-sharing approach for joint matching, pricing, and dispatching using deep reinforcement learning. *IEEE Trans. Intell. Transp. Syst.* **2021**, *22*, 7931–7942. [CrossRef]

25. Kim, S.; Lee, U.; Lee, I.; Kang, N. Idle vehicle relocation strategy through deep learning for shared autonomous electric vehicle system optimization. *J. Clean. Prod.* **2022**, *333*, 130055. [CrossRef]

26. Levin, M.W. A general maximum-stability dispatch policy for shared autonomous vehicle dispatch with an analytical characterization of the maximum throughput. *Transp. Res. Part B Methodol.* **2022**, *163*, 258–280. [CrossRef]

27. Li, L.; Pantelidis, T.; Chow, J.Y.; Jabari, S.E. A real-time dispatching strategy for shared automated electric vehicles with performance guarantees. *Transp. Res. Part E Logist. Transp. Rev.* **2021**, *152*, 102392. [CrossRef]

28. Dai, R.; Ding, C.; Gao, J.; Wu, X.; Yu, B. Optimization and evaluation for autonomous taxi ride-sharing schedule and depot location from the perspective of energy consumption. *Appl. Energy* **2022**, *308*, 118388. [CrossRef]

29. Dean, M.D.; Gurumurthy, K.M.; de Souza, F.; Auld, J.; Kockelman, K.M. Synergies between repositioning and charging strategies for shared autonomous electric vehicle fleets. *Transp. Res. Part D Transp. Environ.* **2022**, *108*, 103314. [CrossRef]

30. Melendez, K.A.; Das, T.K.; Kwon, C. Optimal operation of a system of charging hubs and a fleet of shared autonomous electric vehicles. *Appl. Energy* **2020**, *279*, 115861. [CrossRef]

31. Alqahtani, M.; Scott, M.J.; Hu, M. Dynamic energy scheduling and routing of a large fleet of electric vehicles using multi-agent reinforcement learning. *Comput. Ind. Eng.* **2022**, *169*, 108180. [CrossRef]

32. Zhang, L.; Liu, Z.; Yu, L.; Fang, K.; Yao, B.; Yu, B. Routing optimization of shared autonomous electric vehicles under uncertain travel time and uncertain service time. *Transp. Res. Part E Logist. Transp. Rev.* **2022**, *157*, 102548. [CrossRef]

33. Zhang, T.Z.; Chen, T.D. Smart charging management for shared autonomous electric vehicle fleets: A Puget Sound case study. *Transp. Res. Part D Transp. Environ.* **2020**, *78*, 102184. [CrossRef]

34. Wei, D.; Liu, H. An adaptive-margin support vector regression for short-term traffic flow forecast. *J. Intell. Transp. Syst.* **2013**, *17*, 317–327. [CrossRef]

35. Bi, Z.; Keoleian, G.A.; Lin, Z.; Moore, M.R.; Chen, K.; Song, L.; Zhao, Z. Life cycle assessment and tempo-spatial optimization of deploying dynamic wireless charging technology for electric cars. *Transp. Res. Part C Emerg. Technol.* **2019**, *100*, 53–67. [CrossRef]

36. Chakraborty, D.; Bunch, D.S.; Lee, J.H.; Tal, G. Demand drivers for charging infrastructure-charging behavior of plug-in electric vehicle commuters. *Transp. Res. Part D Transp. Environ.* **2019**, *76*, 255–272. [CrossRef]

37. Ahmad, F.; Alam, M.S.; Shariff, S.M. A cost-efficient energy management system for battery swapping station. *IEEE Syst. J.* **2019**, *13*, 4355–4364. [CrossRef]

38. Yen, J.Y. Finding the k shortest loopless paths in a network. *Manag. Sci.* **1971**, *17*, 712–716. [CrossRef]

39. Available online: http://e-traffic.taichung.gov.tw/RoadGrid/Pages/VD/History2.html (accessed on 3 February 2022).

40. Available online: https://www.psmarketresearch.com/market-analysis/ev-battery-swapping-market/report-sample (accessed on 5 February 2022).

41. Rocha Filho, G.P.; Meneguette, R.I.; Neto JR, T.; Valejo, A.; Weigang, L.; Ueyama, J.; Pessin, G.; Villas, L.A. Enhancing intelligence in traffic management systems to aid in vehicle traffic congestion problems in smart cities. *Ad Hoc Netw.* **2020**, *107*, 102265. [CrossRef]